(4)

Quarterly Letter Report

Growth, Characterization and Device Development in Monocrystalline Diamond Films

Supported by the Innovative Science and Technology Office
Strategic Defense Initiative Organization
Office of Naval Research
under Contract #N00014-90-J-1604
for the period January 1, 1990–December 31, 1992

Robert F. Davis, Klaus J. Bachmann, Jeffrey T. Glass,
D. A. Asbury, M. W. H. Braun, H. S. Kong, Y. H. Lee,
B. R. Stoner, A. Vasudev and B. E. Williams
North Carolina State University
c/o Materials Science and Engineering Department
Campus Box 7907
Raleigh, NC 27695-7907

September 30, 1990

REPORT DOCUMENTATION PAGE

Form Approved
OMB No 0704-0188

1. AGENCY USE ONLY (Leave blank)	2. REPORT DATE	3. REPORT TYPE AND DATES COVERED
	September, 1990	Quarterly Letter 7/1/90-9/30/90

4. TITLE AND SUBTITLE
Growth, Characterization and Device Development in Monocrystalline Diamond Films

5. FUNDING NUMBERS
s400003srr08
1114SS
N00179
N66005
4B855

6. AUTHOR(S)
Robert F. Davis

7. PERFORMING ORGANIZATION NAME(S) AND ADDRESS(ES)
North Carolina State University
Hillsborough Street
Raleigh,NC 27695

8. PERFORMING ORGANIZATION REPORT NUMBER
N00014-90-J-1604

9. SPONSORING/MONITORING AGENCY NAME(S) AND ADDRESS(ES)
Department of the Navy
Office of the Chief of Naval Research
800 North Quincy Street, Code 1513:CMB
Arlington, VA 22217-5000

10. SPONSORING/MONITORING AGENCY REPORT NUMBER

11. SUPPLEMENTARY NOTES

12a. DISTRIBUTION/AVAILABILITY STATEMENT
Approved for Public Release; Distribution Unlimited

12b. DISTRIBUTION CODE

13. ABSTRACT *(Maximum 200 words)*

In this reporting period, diamond films have been deposited on various polycrystalline metal and (001) Si substrates by biased hot filament chemical vapor deposition, the films characterized by TEM, x-ray diffraction and Raman and Auger spectroscopies and devices (specifically IMATTs and MESFETs) modeled from the properties of diamond. Films grown on Si, Ni and W exhibited the highest quality diamond films from the viewpoint of Raman characterization. The model of the MESFET device with gate length = 1 micron and width = 1 mm showed that significant degradation in RF performance is not expected at 10 GHz.

14. SUBJECT TERMS	15. NUMBER OF PAGES
diamond thin films, chemical vapor deposition, Raman spectroscopy, electronic devices, IMPATT, MESFET	48
	16. PRICE CODE

17. SECURITY CLASSIFICATION OF REPORT	18. SECURITY CLASSIFICATION OF THIS PAGE	19. SECURITY CLASSIFICATION OF ABSTRACT	20 LIMITATION OF ABSTRACT
UNCLAS	UNCLAS	UNCLAS	SAR

Preprint: Proc. NATO Advanced Study Institute on Diamond and Diamond-Like Films and Coatings, Castelvecchio Pascoli, Italy, July 23-Aug. 3, 1990.

IN-VACUO SURFACE ANALYSIS OF DIAMOND NUCLEATION AND GROWTH ON SI(111) AND POLYCRYSTALLINE TANTALUM

B.E. Williams, B.R. Stoner, D.A. Asbury, and J.T. Glass

Dept. of Materials Science and Engineering
North Carolina State University
Raleigh, NC 27695-7907

ABSTRACT

A study of both immersed and downstream microwave plasma CVD growth of diamond was accomplished using *in-vacuo* x-ray photoelectron spectroscopy (XPS) and Auger electron spectroscopy (AES) to examine the surface of the sample at selected intervals during different stages of the growth process. Diamond was grown on both Si(111) and polycrystalline tantalum.

INTRODUCTION

The growth of diamond thin films at low temperature and low pressure has made it an excellent candidate material for use in electronic and wear resistant coating applications. However, for diamond to reach its true potential in electronic applications, high quality monocrystalline diamond films must be grown on economically viable non-diamond substrates.

In order to achieve an understanding of the nucleation and growth processes of diamond films on different substrates, we have coupled a diamond growth chamber to an ultrahigh vacuum (UHV) system equipped with a variety of surface analytical techniques including Auger electron spectroscopy (AES), x-ray photoelectron spectroscopy (XPS), low energy electron diffraction (LEED), and electron stimulated desorption (ESD). In this research we stopped the growth at selected intervals and characterized the species present on the surface using XPS and AES without exposure to the air. Specifically, growth of diamond on silicon has been examined as a standard due to numerous reports of CVD of diamond on silicon. Much work has been accomplished on this system, but no study of this nature has been attempted with a microwave plasma CVD growth system. However, since the main interest of the present research is on heteroepitaxial growth of diamond, other substrates (silicon has been shown to be ineffective in this respect) and remote plasma deposition are of greater interest. Therefore, preliminary results for the growth of diamond on polycrystalline tantalum are also reported because single crystal tantalum is a candidate material for heteroepitaxy of diamond.[1] This was done in a remote plasma configuration to minimize ion and electron damage to the surface of the sample.

EXPERIMENTAL

The diamond films examined in this research were deposited using a microwave plasma CVD system. The plasma was formed using a 1 kW microwave source operated at 2.45 GHz with a rectangular waveguide

coupled to a cylindrical cavity. The growth chamber is constructed of stainless steel to be suitable for UHV and has a base pressure of <1 x 10^{-7} Torr when evacuated with the attached turbopump. For growth of diamond films, a controlled mixture of CH_4 and H_2 delivered through mass flow controllers is fed into the chamber using a gas dispersal ring located at the end of the cavity where the waveguide joins the CVD chamber. The desired pressure is controlled by a throttle valve which is attached to a roots blower/mechanical pump assembly. Heating of the substrate is accomplished with an isolated, differentially pumped heating stage. The temperature of the substrate is measured using an infrared pyrometer which was calibrated by melting a bead of high purity aluminum bonded to a silicon wafer. After growth, the sample was cooled under vacuum to a temperature <200 °C before being transferred to the analysis chamber (base pressure 1 x 10^{-10} Torr).

The analysis chamber is equipped with a Riber Mac2 semi-dispersive electron energy analyzer which is used for the XPS and AES measurements. An argon ion sputtering gun is available for cleaning of samples as well as depth profiling. The x-ray source is a dual anode (Mg and Al) source from Riber. The electron source used for Auger is a VG LEG61 which was typically run at 3 kV and 200 μA emission. Acquisition of the XPS and AES data was achieved by controlling the electron analyzer voltages and detection electronics with an IBM AT computer, and the acquisition software was written by one of the authors (Asbury). For XPS, the spectra were obtained by pulse counting using a Riber pulse counter. For AES, standard phase-sensitive detection methods were used to obtain the spectra.

As shown in Figure 1, the analysis chamber and CVD system are connected by a central transfer tube (base pressure = 10^{-9} Torr) which is equipped with a metallization station. Introduction of samples is accomplished via the load lock attached to the transfer tube.

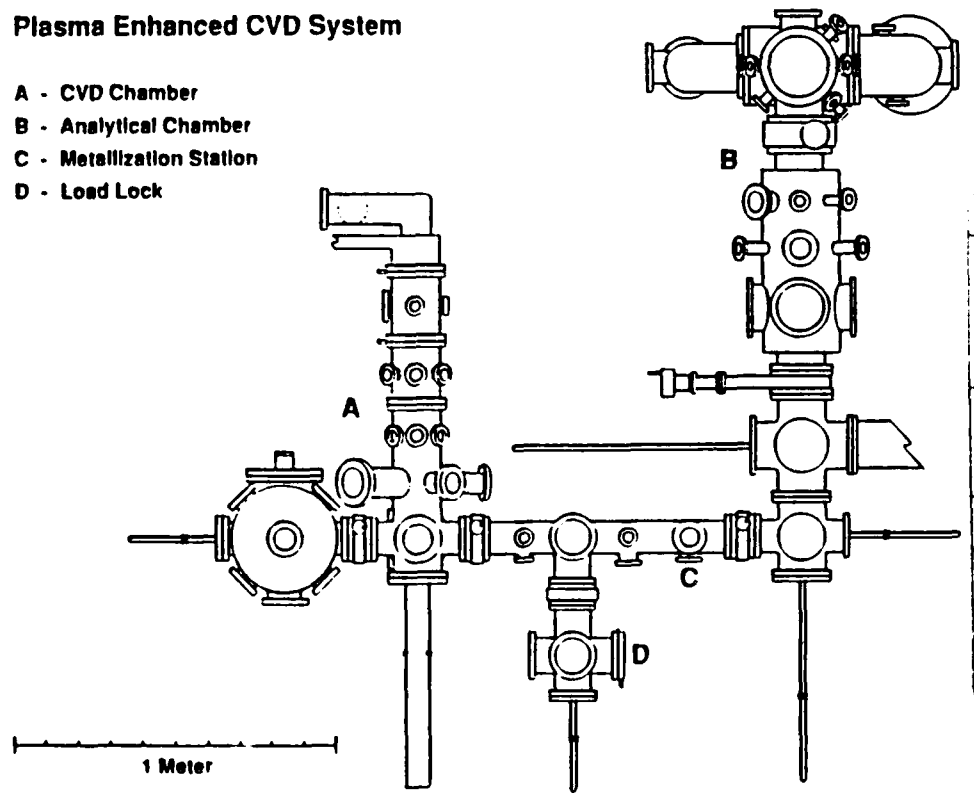

Figure 1 Schematic diagram of microwave plasma CVD chamber and surface analytical chamber.

The preparation of the silicon substrates consisted of an HF etch to strip the oxide from the surface followed by a polish with 0.25 μm diamond to enhance the nucleation density of diamond particles. The

wafer was then cleaned in TCE followed by acetone and ethanol and finally rinsed in deionized water. The tantalum substrates were 10 x 10 x 0.5 mm sheets with a guaranteed purity of at least 99.95%. The sheets were polished using 600 grit SiC paper followed by 6, 3, and 1 μm Al_2O_3 suspended in water. The final polish was accomplished with 0.25 μm diamond paste as used on the silicon substrates. The Ta sheets were then cleaned using TCE, acetone, and ethanol followed by a deionized water rinse.

The growth conditions for the silicon and tantalum substrates are depicted in Table 1. The conditions used for the silicon substrate was used as a standard since the conditions listed are similar to those used in previous research.[2,3] The optimum growth conditions chosen for the tantalum substrate were determined from a parametric study of substrate temperature, pressure, methane concentration, and position relative to the plasma. For this work, the position relative to the plasma is defined as the distance from the edge of the glow discharge to the surface of the sample. The data presented in this research were obtained in the following manner: after exposure to the growth conditions for a given time, the sample remained in the growth chamber until the pressure was reduced to $<10^{-7}$ Torr. Then the sample was transferred to the analysis chamber for XPS and AES approximately 0.5 h after the growth was stopped. The XPS was performed first because previous work on diamond has shown that electron beam exposure can cause changes in the bonding on diamond surfaces. Cycles of growth and analysis on this sample continued until the surface was well covered with diamond.

Table 1. Growth parameters used for silicon and tantalum substrates.

Substrate	Temp. °C	Power (W) For/Rev	CH_4/H_2	Pressure (Torr)	Position relative to plasma
Silicon	800	850/100	1%	25	Immersed
Tantalum	600	850/150	0.5%	25	2.0 cm downstream

RESULTS

Surface Analysis of Diamond on Si (111).

Examination of the Si *2p* region at different growth times can reveal information about its bonding state as the nucleation and growth of diamond occurs. Initially, the Si *2p* indicates a mix of Si-O and Si-Si bonding as shown in Figure 2. The elemental Si *2p* peak at 99.0 eV was used for calibration of the energy scale. The SiO_2 peak is located at 102.7 eV.[4] Thus, prior to growth the silicon substrate is covered by a thin layer of SiO_2 which is expected since the substrate was not cleaned *in-vacuo*. After 0.25 h, some Si-C component is observed as shown by the presence of the new peak located at 100.3 eV. At 0.5 h, more of this carbide component has formed but the elemental Si peak is still dominant. After 1 h, almost all the Si is Si-C bonded. After 5 h, only a trace of Si is observed. The Si-O peak has a nearly constant intensity after the growth is begun, indicating that this Si-O component is confined to the surface. Separate studies have determined that the O component is not due to a leak in the vacuum chamber but rather may be present in the source gas. Efforts to eliminate the source of this oxygen contamination are ongoing.

The value of the C 1s binding energy for pure carbon species (C-C bonding) is not affected by the hybridization of the atoms. That is, the binding energies of graphite and diamond are indistinguishable from one another. However, the presence of the diamond phase on these diamond films was confirmed by other analytical techniques including AES, EELS, and Raman spectroscopy.

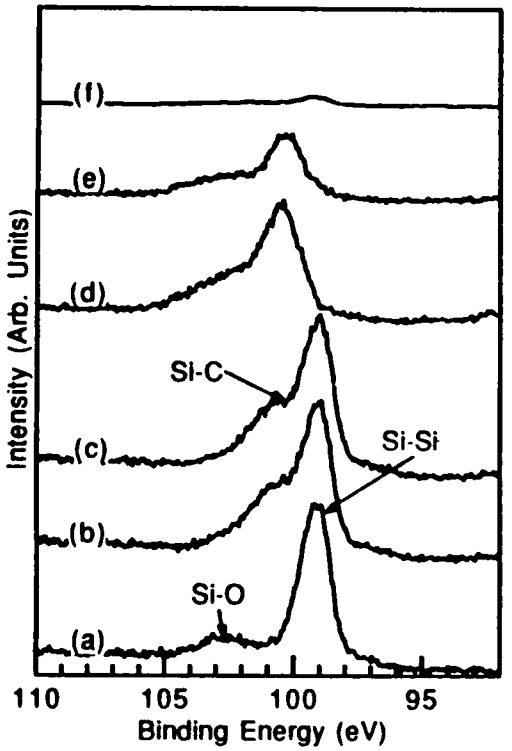

Figure 2 XPS spectra of Si *2p* (a) before growth, (b) at 0.25 h, (c) 0.5 h, (d) 1 h, (e) 2 h , (f) 4 h

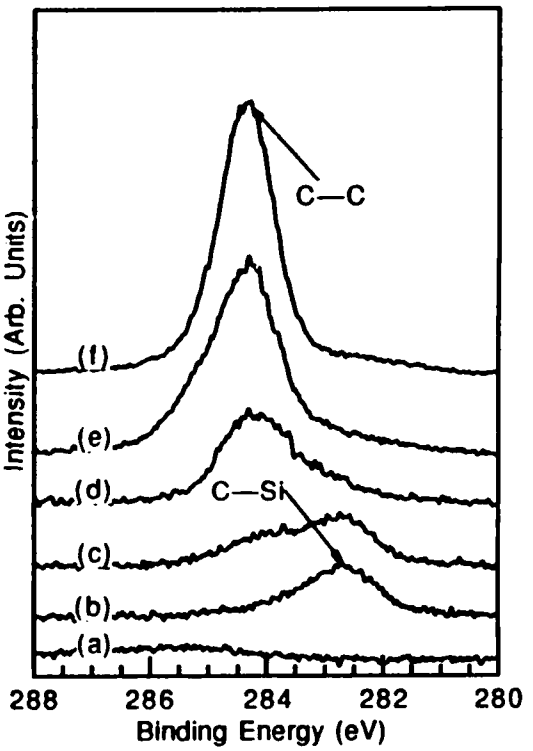

Figure 3 XPS spectra of C *1s* (a) before growth, (b) 0.25 h, (c) 0.5 h, (d) 1 h, (e) 2 h , (f) 4 h

XPS data obtained from the C1s core level at selected growth times is shown in Figure 3. The C observed prior to growth shown in Figure 3(a) is similar to that expected for hydrocarbon contamination on the surface (both C-H and C-O bonding are located at higher binding energy). After 0.25 h, this contamination is reduced and C-Si bonding is observed. After 0.5 h, approximately 40% diamond (C-C) and 60% carbide (C-Si) bonding is observed (determined by area calculation), indicating that nucleation of diamond particles has occurred. In the case of hot filament CVD, Belton found that a complete SiC layer was formed prior to nucleation of diamond particles. In the present work, at 0.5 h the intensity of the elemental silicon peak is higher then that of the SiC peak, indicating that an incomplete layer of SiC has formed, or at least the SiC is in the form of islands. But as observed in Fig.3(c), nucleation of diamond has already been achieved. This means that the diamond particles may be nucleating on silicon and/or SiC as opposed to only nucleating on the SiC as found by Belton. However, the XPS results cannot determine the actual site upon which the diamond is nucleating, but only those species present on the surface. A technique which has spatial capabilities, such as scanning tunneling microscopy, is necessary to determine the answer to this question. After 1 h growth, the C 1s shows an increasing amount of diamond component, and by 5 h only diamond bonding (C-C) is observed.

AES fine structure of the C *KLL* peak has been utilized previously to distinguish the diamond phase from graphite and amorphous carbon.[2,5] Differentiated C *KLL* Auger spectra obtained after different growth times on silicon are shown in Figure 4. After 0.25 h, the fine structure at lower energies of the major C *KLL* peak is indicative of the presence of silicon carbide. This is in agreement with the XPS results and with the results of previous TEM work on diamond growth on silicon. By 1 h, definite changes in the fine structure associated with the C *KLL* have occurred and the spectrum resembles a mix diamond and silicon carbide. The spectrum obtained at 4h has the fine structure expected for a nearly continuous diamond film.

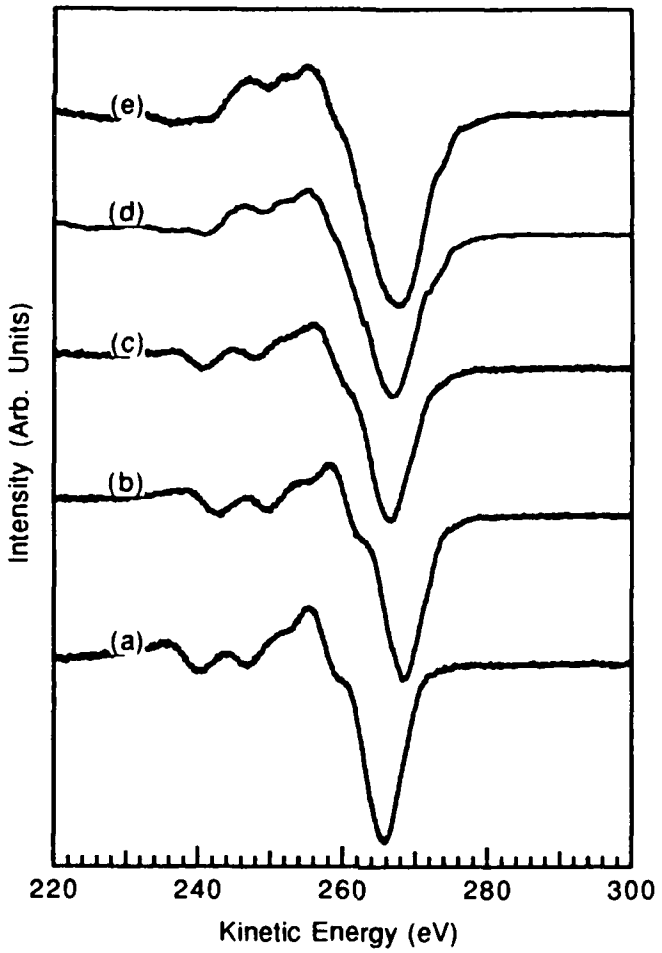

Figure 4 AES of C *KLL* for diamond grown on silicon after growth times of (a) 0.25 h, (b) 0.5 h, (c) 1 h, (d) 2 h, (e) 4 h.

Verification of the diamond phase is further evidenced by the crystalline morphology of the deposited diamond particles. Figure 5 is an SEM micrograph of the diamond film deposited on the silicon substrate. Note the multiple twinning of the particles. This twinning has been examined in detail in previous research and is a result of the structure of the nucleus for the diamond particles.[6]

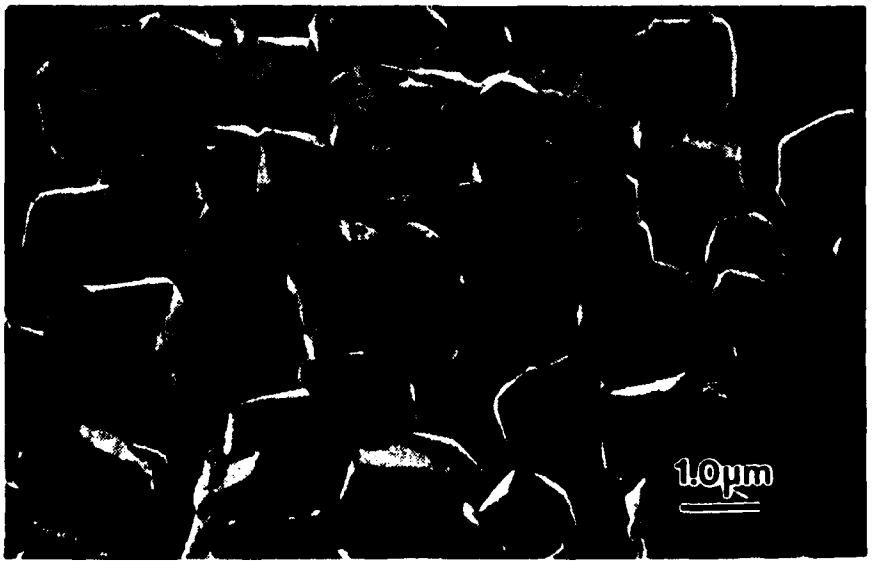

Figure 5 SEM micrograph of diamond film deposited on silicon substrate.

Surface Analysis of Diamond on Polycrystalline Tantalum

Before growth, Fig. 6(a) shows that the Ta substrate is covered by a thin oxide (Ta_2O_5) evidenced by the 4f7/2 binding energy at 26.5 eV. The smaller peak at higher binding energy is due to the 4f5/2 electron as a result of spin orbit splitting in the 4f core level. At lower binding energy, a small peak due to elemental Ta is observed (denoted by Ta on Fig. 6(a). This elemental Ta signal is probably generated from underneath the Ta_2O_5 layer. After only 0.25 h growth, only Ta-C bonding is observed as indicated by the shift to lower binding energy (Ta-C 4f7/2 at 22.6 eV). As the growth continues, the Ta signal decreases. After 5 h, no Ta was detectable by XPS indicating that the coverage of the diamond film was complete and the thickness of the film was sufficient to mask any signal from the underlying substrate.

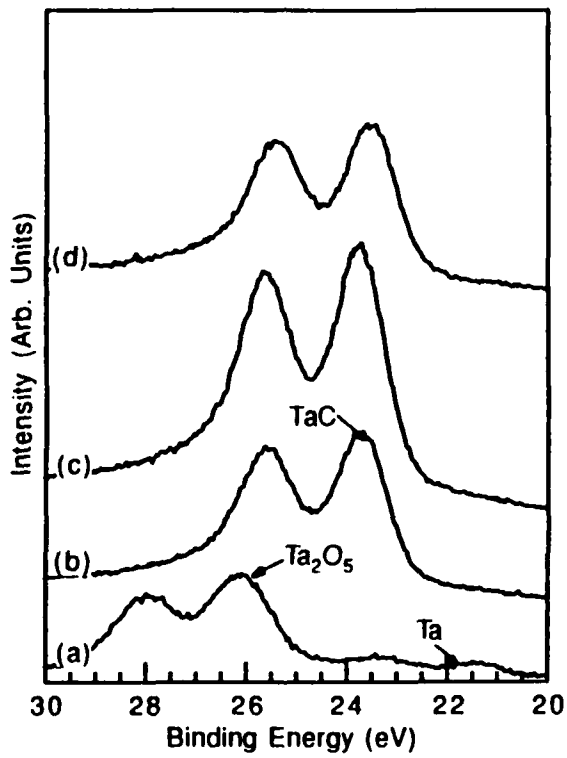

Figure 6. XPS of Ta 4f region at growth times of (a) 0 h, (b) 0.25 h, (c) 0.5 h, and (d) 1 h. Data for 5 h is not shown because no peak was detected.

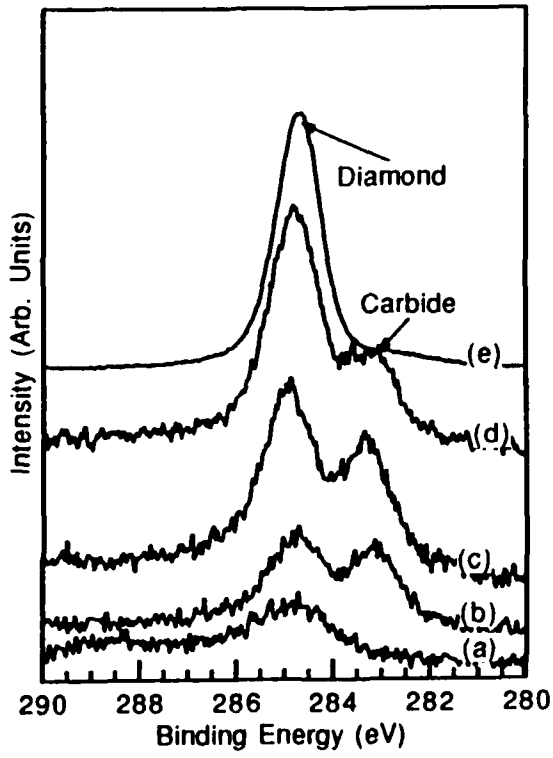

Figure 7. XPS of C 1s for diamond grown on tantalum at growth times of (a) 0 h, (b) 0.25 h, (c) 0.5 h, (d) 1 h, and (e),5 h.

Examination of the C 1s reveals that before growth (Fig. 7(a)) a small amount of carbon contamination is present on the surface, but it is not in the form of a carbide. After 0.25 h, a distinct carbide component is observed at 283.2 eV, while a roughly equal amount of carbon is C-C bonded. As the growth time is increased, the carbide component is reduced while the C-C component increases. At 5 h, a single peak is observed at 284.7 eV, associated with the C-C bonding of diamond.

AES of the C *KLL* after 0.25 h indicates the presence of a carbide (shown by the peaks at lower energy relative to the major peak), in agreement with the XPS observations. As the growth time increases, the peak closest to the low energy side of the *KLL* transition increases in intensity, and the carbide peaks at lower energies decrease in intensity. Finally, after 5 h, the C *KLL* has the shape associated with the diamond phase, and no carbide component is observed.

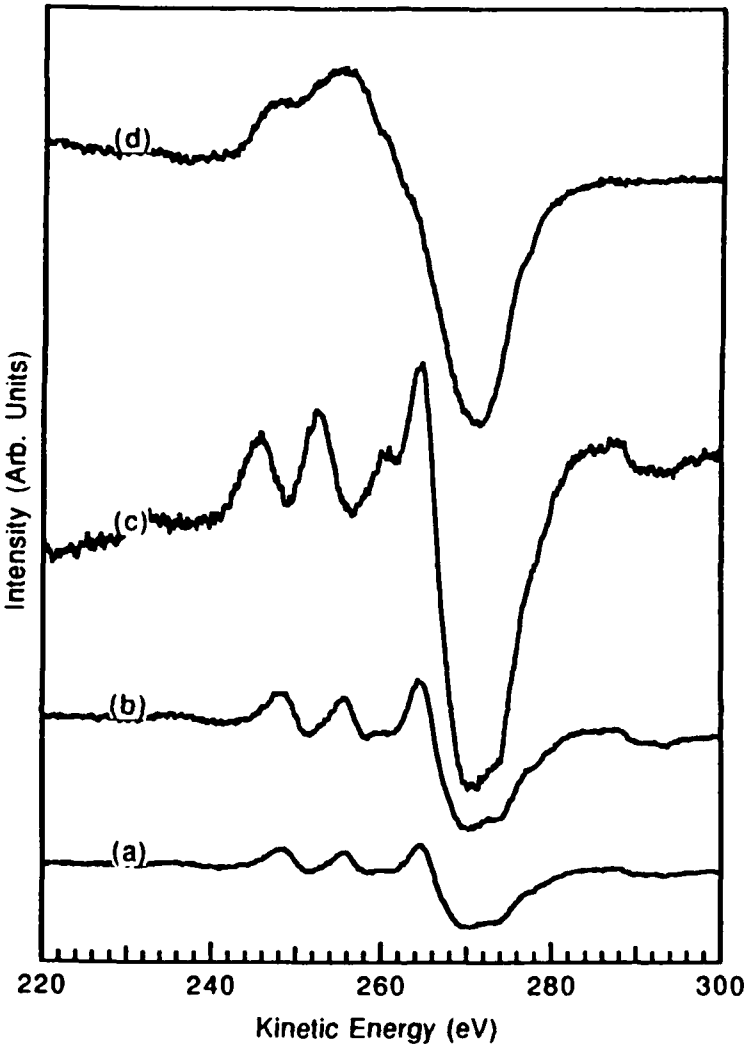

Figure 8. AES of C *KLL* for diamond grown on tantalum at growth times of (A) 0.25 h, (b) 0.5 h, (c) 1 h and (d) 5 h.

The morphology of the diamond film after 5 h growth can be seen in the SEM micrograph shown in Fig. 9. The (111) faceting is typical of high quality diamond films reported in the literature. The crystal size is small relative to silicon, indicative of a high nucleation density. The thickness of this diamond film is less than 1 μm and the film is transparent when viewed through an optical microscope.

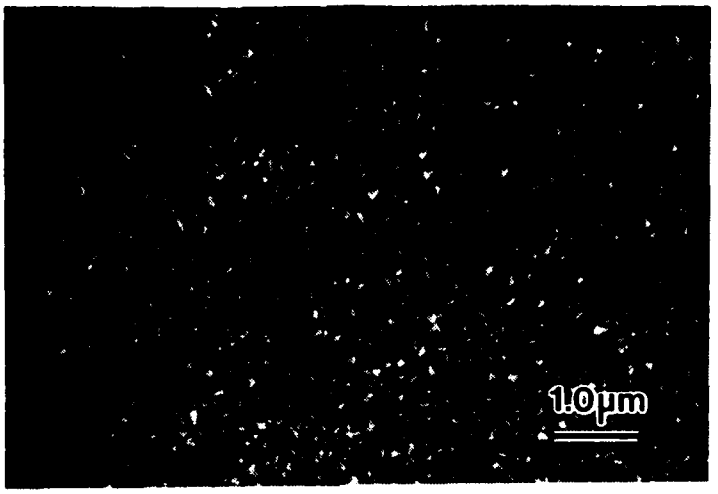

Figure 9. SEM micrograph of diamond film grown on tantalum substrate.

CONCLUSIONS

In-vacuo surface analysis of diamond grown on silicon substrates has shown that at first the silicon substrate is covered by a thin layer of oxide and some hydrocarbon contamination. After 0.25 h growth, SiC is formed at the expense of some of the native oxide observed prior to growth. However, oxygen is still present (as observed in survey spectra), probably at the surface of the newly grown SiC. After 0.5 h, the presence of diamond is detected, apparently before a complete film of SiC has formed. After 4 h growth the surface is nearly covered by diamond particles. Oxygen contamination of surfaces has been observed, but the source of this contamination has not yet been determined.

Diamond growth has also been achieved in a downstream mode on polycrystalline tantalum substrates. This method may be more suitable for heteroepitaxy since the crystallinity of the substrate may be affected by the ion and electron bombardment from the plasma. XPS and AES indicate that for diamond growth on tantalum, a layer of tantalum carbide is formed very rapidly (<0.25 h). The diamond then nucleates and grows on this tantalum carbide layer.

ACKNOWLEDGMENTS

Support from SDIO/IST through ONR and partial support of the Kobe Steel Ltd. Professorship is gratefully acknowledged. Useful technical discussions with D. Belton and R. F. Davis are also appreciated. T. Tachibana, S. Wolter, and A. Mundsen have provided invaluable assistance in the laboratory.

REFERENCES

[1]Y. H. Lee, P. D. Richard, K. J. Bachmann and J. T. Glass, Appl. Phys. Lett. 56, 620 (1990).

[2]B. E. Williams and J. T. Glass, J. Mater. Res. 4, 373 (1989).

[3]K. Kobashi, Phys. Rev. B 38, 4067 (1988).

[4]D. N. Belton, S. J. Harris, S. J. Schmieg, A. M. Wiener and T. A. Perry, Appl. Phys. Lett. 54, 416 (1989).

[5]P. G. Lurie and J. M. Wilson, Surf. Sci. 65, 476 (1977).

[6]B. E. Williams, J. T. Glass, R. F. Davis, K. Kobashi and Y. Kawate, MRS Proc. (1988).

SUBSTRATE EFFECTS ON THE GROWTH CHARACTERISTICS AND ELECTRICAL PROPERTIES OF VAPOR DEPOSITED POLYCRYSTALLINE DIAMOND THIN FILMS

Y.H. LEE*, K.J. Bachmann and J.T. Glass
North Carolina State University, Materials Science and Engineering Department, Raleigh, NC 27695-7907
* Present Address: Samsung Electronics, Semiconductor Division, C.P.P. Box 8780, Seoul, Korea

ABSTRACT

The growth of diamond films on clean Si(001), Ni(001), Mo(111), Ta(111) and W(111) substrates at low defect density by bias controlled chemical vapor deposition is discussed. Three-dimensional growth by the Volmer-Weber mechanism dominated on these substrates with relatively low nucleation rate as compared to scratched silicon substrate surfaces. The aspect ratio of diamond grown on single crystals of different substrate materials correlates with their surface free energies. The electrical properties of polycrystalline diamond films grown on Si and Al_2O_3 substrates depended strongly on the residual sp^2 bonding with Si being a favorable substrate for controlling the electrical behavior under the conditions of bias controlled CVD.

INTRODUCTION

Diamond has several properties that make it an attractive semiconductor material for high-power, high-speed and high-temperature electronic devices. These properties include high thermal conductivity 2,000 W/k/m which is five times that of Cu at 20°C, wide band gap (~5.4eV), high electron and hole mobilities of 2200 and 1600 $cm^2/V/$ sec, respectively, high breakdown fields (10^7 V/cm) and radiation hardness. Consequently, a considerable effort has been spent on fabricating bulk and homoepitaxial diamond devices.[1-4] However, economic considerations limit the use of homoepitaxy in technology oriented research and development, so that heteroepitaxial diamond thin films on readily available substrate materials are of primary interest for device oriented research.

EXPERIMENTAL CONDITIONS

Diamond Growth on Various Single Crystal Substrates

Diamond thin films were grown on Si(001), Ni(001), Mo(111), Ta(111) and W(111) by BCCVD process as described in more detail in references (5,6). These single crystal metal substrates were prepared very carefully to avoid damage to the surface by utilizing spark-erosion slicing, 9μm, 5μm, 1μm, 0.1μm alumina polishing followed by 2 hours of polishing in a colloidal silica solution [6]. These substrates were chosen for the following reasons: (i) Si is a material with the diamond structure and has an excellent thermal expansion match with diamond. (ii) Ni is closely lattice-matched to diamond, (iii) refractory metals such as Mo, Ta, W are strong carbide formers with relatively high surface energies (i.e., relatively close to diamond) and thus are expected to result in stronger bonding of the diamond nuclei than on Cu or Ni.

Substrate Effects on Electrical Properties

Polycrystalline Al_2O_3 and n-type phosphorous doped (001) Si were employed as substrate materials. Al_2O_3 substrates were chosen due to their high resistivity ($>10^{13}\Omega$cm) which allowed electrical measurements to be made without any electrical contribution from the substrates. The films were deposited on the substrates under reverse bias of 150 V for 6 hrs and 10 hrs, respectively. The thickness of the films obtained was approximately 2μm with highest growth rate on the Al_2O_3 substrate. Although these films were not doped intentionally, a boron concentration of ~$4.0x10^{18}/cm^3$ was measured in these films by SIMS due to the BN substrate support used in the system and resulted in p-type conduction.[7,8] After diamond deposition, samples of 5mm x 5mm dimensions were cut using a diamond saw followed by solvent cleaning in TCE, Acetone, and Methanol, and etching by hot concentrated H_2SO_4 at ~70°C for 10 minutes. A final cleaning was carried out using a 1:1 mixture of H_2SO_4 and H_2O_2. Specimens were then dried in an oven at 120°C for 5 minutes to eliminate moisture on the diamond films.

A layer of Pt, 2000Å in thickness, was deposited onto the samples to form a metal-semiconductor contact by rf sputtering. The rf power was 100W and the gas pressure was 10 millitorr. By employing photolithography and lift-off, 100μm diam. active device areas were delineated. These active devices were separated from the field region by a 100μm wide annular ring. Electrical grounding was made on the same side of the sample. The structure of these diodes were similar to that reported by Ioannou et al.[9,10] Measurements of I-V characteristics between the active device and the field region was conducted using an HP 4145A semiconductor parameter analyzer.

RESULTS AND DISCUSSION

Diamond Growth on Various Single Crystal Substrates

The growth of diamond films on clean Si(001), Ni(001), Mo(111), Ta(111), and W(111) has been accomplished. Three-dimensional growth by the Volmer-Weber mechanism dominated on these substrates with relatively low nucleation rate ($< x 10^5$ sites/cm^2) as compared to scratched silicon substrate surfaces. For heteroepitaxy of diamond thin films, it is necessary to obtain 2-dimensional or at least high aspect ration in the lateral growth by (i) the surface energy of the diamond decreased or the surface energy of the substrate increased, and/ or (ii) the interaction between C atoms and the substrate increased. Therefore, an attempt was made to check the feasibility of such considerations for the present research. The surface free energy of diamond is estimated to be 3387 ergs/cm^2,[11] while the surface free energies of Si, Ni, Mo, Ta, and W are 1457 ergs/cm^2, 2072 ergs/cm^2, 2463 ergs/cm^2, 2628 ergs/cm^2 and 3111 ergs/cm^2, respectively.[12] Figure 1 shows the morphologies of diamond nuclei on single crystal substrates with different surface energies. It is observed that the aspect ratios of the diamond nuclei (i.e., the length of the nuclei parallel to the substrate versus the height of the particle perpendicular to the substrate) correlate to the surface energies for the substrates except in the case of Si, and Ta. That is, lower, flatter particles are observed on W, Mo, and Ta rather than on the Si and Ni substrates. Although Ta yielded a somewhat lower aspect ratio than expected, it may be attributed to the formation of two different types of carbides on the Ta surface; diamond nuclei need additional energy to overcome the boundary between domains of different carbides with different structures and continue lateral growth.[6] On Si, relatively extended lateral growth is observed which can be attributed to either the formation of a interfacial layer with higher surface energy (such as W_5Si_3 or SiC) and/or the higher interaction with carbon atoms than Ni which would result in an increase in adsorption energy.

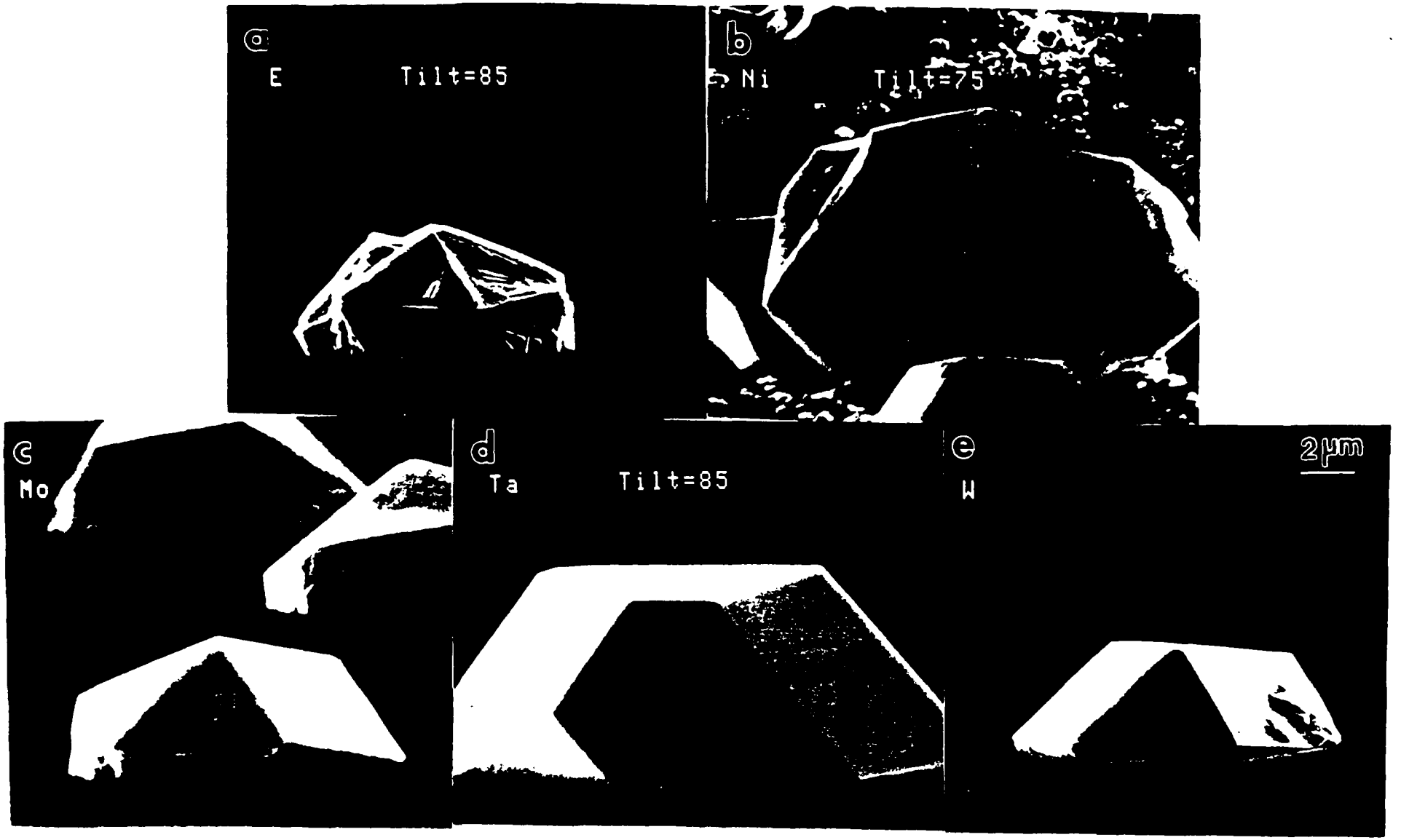

Figure 1. The morphologies of diamond nuclei viewed at θ=85° (θ=75° for Ni) on (a) (001) Si (b) (001) Ni (c) (111) Mo (d) (111) Ta (e) (111) W.

Substrate Effects on Electrical Properties

Figure 2 shows the surface morphology of B doped diamond films grown on Al_2O_3 and n-(001)Si substrates. It is observed that clear (001) facets are dominant on Si(001) substrate while five fold multiply twinned particles are dominant on Al_2O_3 substrate. The corresponding Raman spectra of the samples are shown in Figure 3. As seen by the I_D/I_G ratios and the FWHM (Table 1), diamond films of excellent quality with only a very small sp^2-bonded components were obtained on Si substrate, while poor quality diamond films with substantial amounts of sp^2-bonding were obtained on Al_2O_3 substrate. The current-voltage characteristics of the metal-semiconductor contact diodes fabricated on diamond films on polycrystalline Al_2O_3 and (001) Si substrates are shown in Fig. 4 a and b, respectively. The plot in Fig. 4a shows an approximately linear characteristics indicating a high leakage current which is believed to be due to the substantial amount of carbon sp^2-bonding in these films.

In contrast, the plot in Fig. 4b show asymmetric (rectification) behavior as expected for 2 Schottky diodes of substantially different surface area connected back to back. From the direction of the reverse current for the smaller diode, the polarity of this film was determined to be p- type. The leakage current stays relatively low for reverse biases up to 30V. It was not possible to reliably measure the resistivity of the diamond films on Si due to the conductive nature of the Si substrates. Nonetheless, the minimum value of the resistivity has been measured to 330Ωcm utilizing four point probe techniques which compares to 20Ωcm resistivity of the films grown on Al_2O_3.

TABLE 1. The corresponding Raman parameters of the diamond films shown in Fig. 3.

Substrate	FWHM	I_D / I_G	Film Resistivity (Ω-cm)
Al_2O_3	15 cm^{-1}	2.86	20
n-(001) Si	4.2 cm^{-1}	40	>300

SUMMARY AND CONCLUSIONS

Diamond thin films were grown on Clean Si(001), Ni(001), Mo(111), Ta(111) and W(111) substrates. It has been shown that the morphologies of diamond particles on different substrate materials is in accord with the relation between surface energy of the substrates relative to the surface energy of diamond as predicted by classical crystal growth theory. Substrates which have surface energies closest to diamond yield the most extended lateral growth.

Diamond films were also grown on Si(001)substrates and polycrystalline Al_2O_3 substrates under reverse bias of 150V. Electrical properties of diamond films are strongly

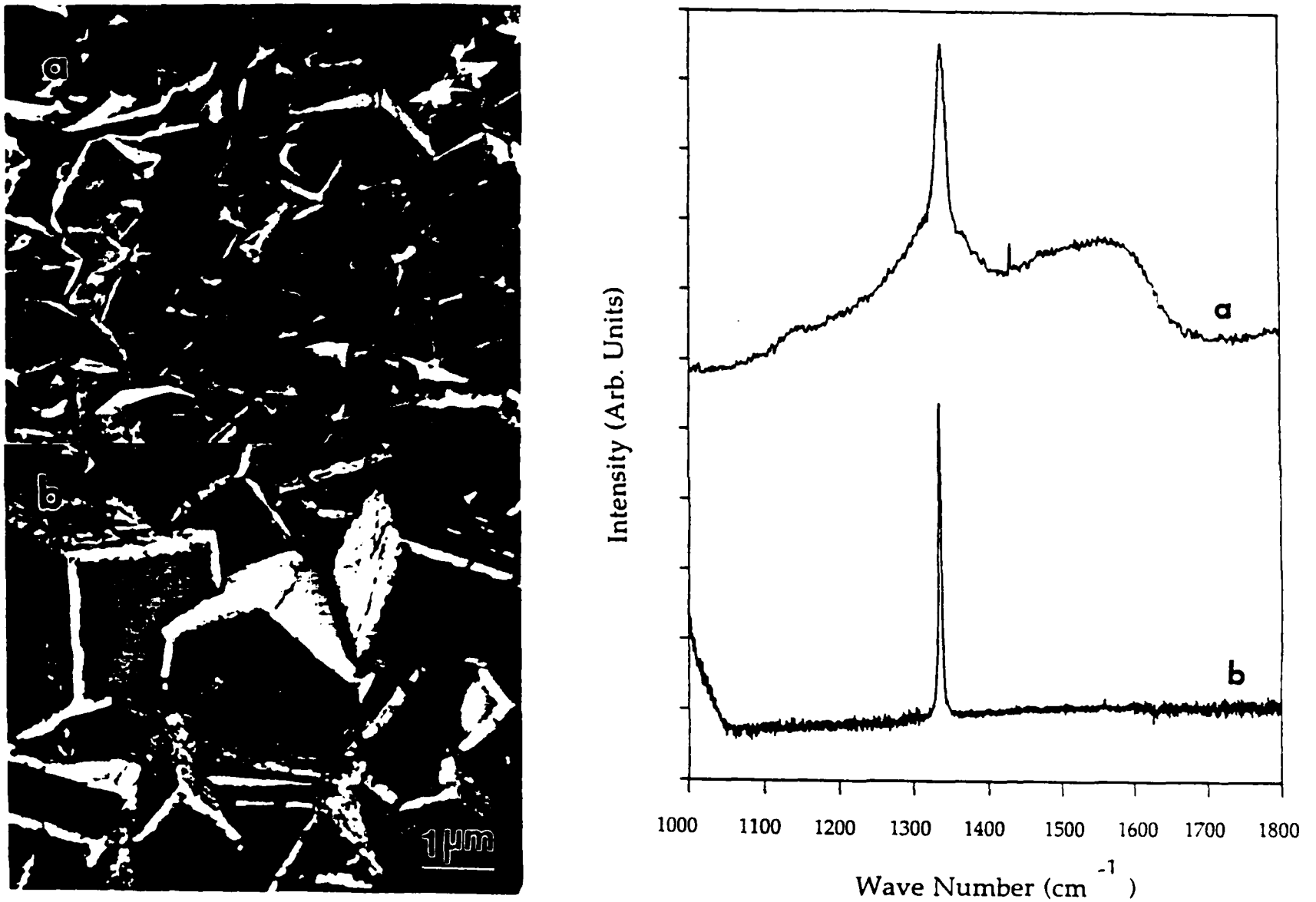

Figure 2. Surface morphologies and corresponding Raman Spectra of diamond films grown by BCCVD on (a) Al_2O_3 substrate (b) n-(001)Si substrate.

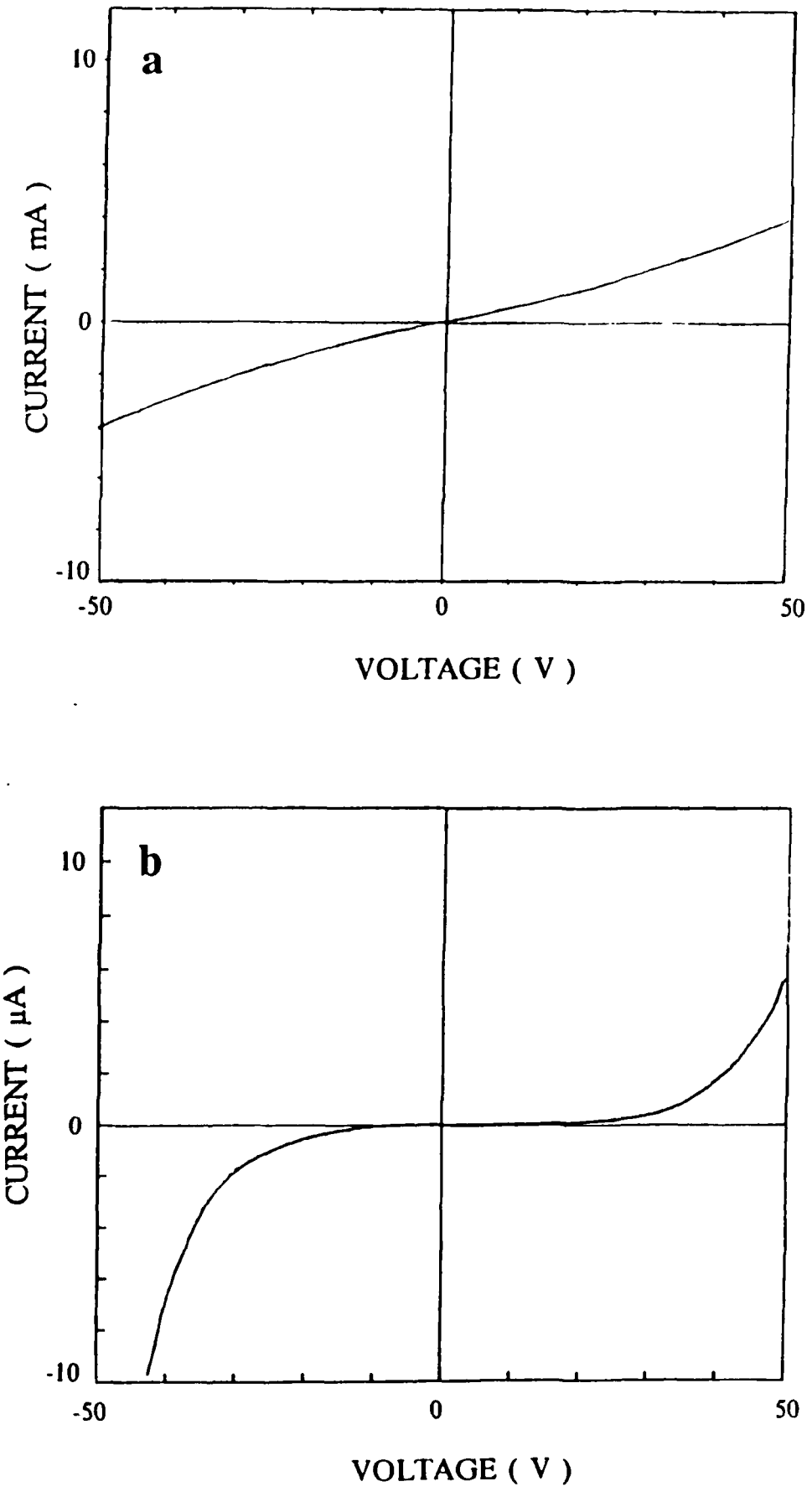

Figure 3. Typical I-V characteristics of the diamond film with Pt electrodes at room temperature. The sample designations are the same as Figure 2.

Submitted to:
Journal of Applied Physics on August 16, 1990.
Their reference, R-8038; received Aug 22,1990.
Subject Classification: 68.55

THE ROLE OF GEOMETRIC CONSIDERATIONS IN THE DIAMOND-CUBIC BORON NITRIDE HETEROEPITAXIAL SYSTEM

MWH Braun[1], HS Kong, JT Glass and RF Davis,

Dept of Materials Science and Engineering, North Carolina State University, USA

ABSTRACT

A geometric criterion for minimization of interfacial energy when crystals grow together on a planar epitaxial interface formulated in reciprocal space is applied to the Diamond - cubic Boron Nitride [BN_{cub}] heteroepitaxial system. It was found that low index like planes require a relatively small strain of 1.37% from bulk parameters. The unlike epitaxial configuration which pairs Diamond {100} with BN_{cub}{221} yields two dimensional coincidence with the same small strain and is favoured above other low index mixed configurations in this way. The agreement between this epitaxial criterion and the experimentally observed behavior reported in the literature is encouraging, and motivates a search for further systems with this technique.

INTRODUCTION AND BACKGROUND

Due to its unique combination of properties, diamond has significant potential as a high power/moderate-to-high frequency device material or for devices to be operated in high temperature or radiation intensive environments. Such potential is derived from the unique combination of properties including high thermal conductivity, large breakdown voltage, high electron saturated drift velocity and reasonably high carrier mobilities[2-4]. Unfortunately, the scarcity and expense of semiconducting bulk single crystal diamonds has limited their usefulness. However, with the recent development of the vapor phase deposition of diamond[5-11], interest has been renewed in this area although several significant hurdles remain to be overcome. Perhaps the most significant of these is the growth of single crystal diamond films on economically viable non-diamond substrates. Most diamond films consist of a rather small polycrystalline morphology due to poor film-substrate lattice matching and the very high surface energy of diamond which causes three-dimensional, particulate nucleation and growth. The two notable exceptions to this are diamond deposition on diamond and on cubic Boron Nitride [BN_{cub}].

In the case of diamond substrates, smooth surfaces containing step features are generally observed[12,13] indicating oriented lateral growth. This implies good lattice match as well as satisfaction of the surface energy criteria as is expected in homoepitaxy. For the growth of diamond on BN_{cub}[14,15,16], an oriented three-dimensional island growth is observed which leads to a single crystal film after the islands coalesce. This indicates that the lattice matching is reasonably good (i.e., relatively low strain energy) but that free energy is not minimized to yield lateral growth. This may be due to a combination of a surface energy mismatch between the substrate and the film as well as the finite misfit strain energy. Nonetheless, a single crystal diamond film has been achieved on cubic Boron Nitride, thus proving the feasibility of heteroepitaxial growth. Unfortunately, BN_{cub} substrates are more difficult to obtain than bulk diamond. Therefore this advancement is rather academic. To

translate this scientific achievement into an application, it is necessary to conduct a detailed examination of the diamond-BN_{cub} system in order to understand the reasons for the success of this heteroepitaxial growth. This will allow the proper choice of other substrate materials and orientations which have potential for achieving heteroepitaxial growth of diamond.

In view of this a general epitaxial criterion first obtained and formulated in reciprocal space by Fletcher[17] and derived by other means and extended by Braun[18,19] has been utilized in the present manuscript to examine this system. It is found that the reported observations of this system agree well with the reciprocal space considerations. It is conjectured that the rigidity of Diamond makes the agreement with the geometric matching requirement a strong necessary condition for epitaxy. This would enable the selection of candidate substrates for heteroepitaxy with Diamond.

This paper briefly reviews the principles of the interfacial energy considerations in terms of the Van der Merwe-Reiss rigid model[20,21] and follows a derivation given by Braun of the epitaxial criterion formulated in reciprocal space. It further reviews the reciprocal space and direct space consequences of the criterion. These considerations are then applied to the matching conditions of the low index like faces of Diamond and cubic Boron-Nitride as well as the mixed face pairs of Diamond {100}, {110}, {111}, {112}, {114} and {120} on BN {221} and Diamond {110} on the BN{120} face, Diamond {100} on BN{110}, and Diamond {100}, {110} and {111} on the BN{112} faces. Some unique aspects of the Diamond {100}, BN{221} pair are highlighted.

ENERGIES CONCERNED IN EPITAXY

Several models which give the energy of the bicrystal subject to various approximations have been used to predict epitaxial orientations or interfacial structure[17,20-24]. Inherent to them is

the assumption that epitaxial orientations minimize the Gibbs free energy of the system, a condition usually approximated by minimizing the bicrystal energy itself.

The equilibrium condition for the growth of an epitaxial monolayer (O) on a substrate crystal (S) has been formulated in terms of three contributions to the free energy change on formation of the monolayer as the inequality[25,26]

$$\Delta\gamma_{OS} \equiv \gamma_O - \gamma_S + \gamma_I \leq 0 \qquad (1)$$

where γ_O and γ_S are the surface energy of the overgrowth and substrate respectively, and γ_I is the energy associated with the formation of the interface. In the presence of misfit this last term contains the elastic strain energy in the monolayer and misfit energy of interfacial disregistry. The final epitaxial configuration will be largely a result of the competition between these contributions to the energy. This energy contribution increases with island size, so that the monolayer condition may be violated beyond a critical island size. As a consequence the condition may be coupled to the growth mode expected, observed, or simply hoped for. When the inequality is violated, the overlayer grows three dimensionally in the form of islands, (Volmer-Weber growth mode), while satisfied it grows in a monolayer-by-monolayer mode (Frank-van der Merwe mode). The interfacial energy is naturally zero when the overgrowth and substrate are the same material and misfit is absent as in a homoepitaxial system.

The values of the first terms are given by the growth conditions, materials, etc, and very little can be done to avoid their effects beyond growing under non-equilibrium conditions. Techniques involve the use of surfactants during growth, to directly change the chemical potential contributing to the free energy, or keeping the substrate at a low temperature, to prevent atoms from reaching their equilibrium position on top of a growing island, rather than

at its edge. In the latter case the observed growth proceeds via an island mechanism, but these rapidly grow together to none the less form a continuous film.

The third term in eq. (1) contains the geometric parameters which determine whether a film grows epitaxially, and the resulting orientation. The associated energy contributions can be modelled effectively with models of the Frank-van der Merwe type[20,21,28-32]. However these models generically suffer from the lack of knowledge of the values of explicit energy parameters, such as overlayer-substrate bonding strengths and elastic constants as applicable to monolayer or thin systems, but have been successful in qualitatively explaining the behavior of epitaxial systems.

This paper seeks to address the contributions to the interfacial energy by geometric factors, specifically surface unit cell periodicity, the orientations of the component crystals and the various measures of quality which correlate with the achievement of epitaxy. Specifically, by considering the energy due to lattice mismatch, a geometric criterion is derived which is conveniently formulated in the reciprocal lattices of the two crystal surface systems.

In the absence of knowledge of either the exact misfit energy or the precise elastic constants, only necessary conditions can be determined, and quality factors defined to rank various possible configurations. These are however essentially geometric factors, which make it possible when selecting candidate systems for epitaxial growth to not only use surface energy values, but also to address the epitaxially orienting term in a simple and effective manner.

THE EPITAXIAL CRITERION

In the geometric limit both components of the bicrystal are considered rigid, retain their bulk lattice structures and parameters and are in contact at a single interfacial plane. On either

side of the interface each component crystal presents a crystal plane with unique translational and rotational symmetries. The periodicities are described by infinite sets of wave vectors which form the surface reciprocal lattices for each crystal face.

The interaction energy between individual interfacial overgrowth atoms (adatoms) and the substrate surface is assumed to be dependent on position and is given in Fourier form as the potential

$$V(x,y) = \sum_{\{\mathbf{q}\}} V_{\mathbf{q}} \exp(i\mathbf{q}\cdot\mathbf{r}) = \sum_{h,\,k=-\infty}^{\infty} V_{hk} \exp[i2\pi\,(hx+ky)] \qquad (2)$$

where $\mathbf{q} = h\mathbf{a}_1^* + k\mathbf{a}_2^* \equiv \mathbf{q}_{hk}$ is a lattice translation vector of the substrate surface reciprocal lattice (defined by the condition $\mathbf{a}_i \cdot \mathbf{a}_j^* = 2\pi\delta_{ij}$, i,j = 1,2) and h and k are required to be integers. In this expression, $V_{\mathbf{q}}$ and V_{hk} are Fourier coefficients appropriate to the two equivalent forms of the series. Position in the substrate surface lattice is given by $\mathbf{r} = x\mathbf{a}_1 + y\mathbf{a}_2$, where $\mathbf{a}_1$ and $\mathbf{a}_2$ are basis vectors of the substrate surface unit cell.

An overgrowth island is constructed to contain (2M+1)×(2N+1) overgrowth lattice points. These are arranged as 2N+1 rows of 2M+1 points each, and are obtained by displacing a single (central) point by all the vectors in the set

$$\{\mathbf{r}_b = m\mathbf{b}_1 + n\mathbf{b}_2 : m = -M, \ldots 0, \ldots M;\ n=-N, \ldots 0, \ldots N\} \qquad (3)$$

where $\mathbf{b}_1$ and $\mathbf{b}_2$ are basis vectors of the overgrowth surface unit cell. The limit as $M,N \rightarrow \infty$ describes a monolayer.

It is assumed here, without loss of generality, that the origin of the overgrowth lattice is placed at a minimum of energy in the substrate potential, (eq. 2) and that this is also chosen as the origin of the substrate lattice. The energy scale is chosen in such a way that if every overgrowth atom lies at an exact minimum of the substrate, the total energy given by expression (2) will be zero. Any deviation from this exact matching situation (*misfit* then exists) yields an energy greater than zero. With this choice the energy is interpreted directly as *misfit energy*. While a quantitative model would require that the Fourier coefficients in eq. (2) actually have values, and would normally require truncation of the series after a few terms, the geometric considerations here do not require that any values are assumed.

After summing individual energy contributions over all the atoms in the overgrowth island, the total interaction energy *per atom* for G overgrowth atoms is seen to be

$$V_a = \frac{1}{G} \sum_{h,k} V_{hk} \frac{\sin \pi(2M+1)p(h,k)}{\sin \pi p(h,k)} \cdot \frac{\sin \pi(2N+1)q(h,k)}{\sin \pi q(h,k)} \qquad (4)$$

An obvious generalization additionally treats the substrate in the field of the overgrowth system as experiencing a misfit energy similarly expressible as a Fourier series as eqs. (2) and (4), but summed over the reciprocal lattice vectors of the overgrowth. The total misfit energy (per atom) is then given by[20,18]

$$V_{mis} = \frac{1}{2}(V_a + V_b) \qquad (5)$$

The rather distinctive sine expressions of eq (4) also occur in the standard derivation of the von Laue condition in x-ray crystallography, (see for example the text by Busch and

Schade[27], or Kittel[28]) and are in fact obtained here in an analogous summation process. This is to be expected since in both x-ray diffraction theory and here, the contributions to some quantity, (amplitude in diffraction, misfit energy respectively) from two periodic systems are being added, and qualitatively similar resonance conditions are expected.

The relationship between the pairs p, q and h, k is given by the expressions

$$p(h,k) = hr_{11}\, c_\theta + kr_{12}\, s_\theta \quad , \qquad q(h,k) = hr_{21}\, s_{\theta\beta} + kr_{22}\, c_{\theta\beta} \tag{6a}$$

with θ the angle between $\mathbf{b}_1$ and $\mathbf{a}_1$ and

$$r_{ij} = b_i/a_j = C_{bi}\, b_{nn}/C_{aj}\, a_{nn} = (C_{bi}/C_{aj})r \quad , \qquad r = b_{nn}/a_{nn} \quad , \qquad i,j = 1, 2 \tag{6b}$$

$$c_\theta = \sin(\alpha-\theta)/\sin\alpha \quad , \qquad s_\theta = \sin\theta/\sin\alpha \, ,$$

$$s_{\theta\beta} = \sin(\alpha-\beta-\theta)/\sin\alpha \quad , \qquad c_{\theta\beta} = \sin(\beta+\theta)/\sin\alpha$$

while r is termed the ratio of nearest neighbor distances, a_{nn} and b_{nn}, or simply the nearest neighbour ratio. This identifies with the atomic size ratio introduced by Bruce and Jaeger.[29]. Other quantities are the substrate and overgrowth surface unit cell angles, α and β, and the lengths of the surface cell basis vectors, a_i and b_i.

Direct calculation of the transformation between the $\mathbf{b}_1$, $\mathbf{b}_2$ and $\mathbf{a}_1$, $\mathbf{a}_2$ systems shows that p(h,k) and q(h,k) are the overgrowth reciprocal lattice coordinates of the substrate wave vector $\mathbf{q}_{hk}$. The energy in eq. (3) peaks sharply when p and q are integers. When this necessary condition is met the misfit energy is sharply minimized when the product of the sine terms and the resonating V_{hk} is negative. Translation of the origin of the overgrowth in the substrate unit cell to (x_o, y_o) introduces a factor $F^o = \exp(i\mathbf{q}_{hk}\cdot\mathbf{r}_o) = \exp[i2\pi(hx_o+ky_o)]$

and a factor of this type may be introduced to invert the sign (but implies displacement of the island).

This means that a translation vector of the substrate reciprocal lattice $\mathbf{q}_{hk}$ *must coincide with a translation vector of the overgrowth reciprocal lattice,* $\mathbf{q}^{pq}$, *where* p *and* q *are integers.*

Hence, the condition

$$\mathbf{q}_{hk} = \mathbf{q}^{pq} \tag{7}$$

defines a *necessary* condition for an *ideal epitaxial configuration.* This is defined as an orientation and associated nearest neighbour ratio at which the interfacial misfit energy is minimized for a rigid system with these structures[18]. At equilibrium, systems with ideal lattice parameters will be found in the orientation yielding the least interfacial energy. This reciprocal space condition has previously been obtained from a different model by Fletcher[17]. It is analogous to the von Laue condition of crystallography.

Reciprocal lattice vectors in two dimensions propagate line wave fronts which coincide with rows of lattice points. The spacing of such rows of lattice points is given by the wavelengths of the propagation vectors, while the direction of the wave vectors is perpendicular to the lattice rows. The spacing of the rows propagated by vector $\mathbf{q}_{hk}$ is given by

$$\lambda_{hk} = \frac{2\pi}{|\mathbf{q}_{hk}|} = \frac{2\pi}{\sqrt{h^2\mathbf{a}_1^*\cdot\mathbf{a}_1^* + 2hk\mathbf{a}_1^*\cdot\mathbf{a}_2^* + k^2\mathbf{a}_2^*\cdot\mathbf{a}_2^*}} \tag{8}$$

In analogy to the zone law, it is always true that

$$h\mathbf{a}_1^* + k\mathbf{a}_2^* \perp k\mathbf{a}_1 - h\mathbf{a}_2 \qquad (9)$$

from which the lattice directions of matched rows are obtained directly.

Consequences of the coincidence of a pair of overgrowth and substrate reciprocal lattice vectors may be listed as follows:

i) If the wave vectors are parallel, then so are the lattice rows they propagate. This means that when crystals are aligned in an ideal epitaxial orientation, lattice rows of substrate and overgrowth are aligned in parallel orientation.

When a pair of vectors is not parallel, the magnitude of the necessary angle of rotation is given by

$$\cos \theta_R = \frac{\mathbf{q}^{pq} \cdot \mathbf{q}_{hk}}{|\mathbf{q}^{pq}||\mathbf{q}_{hk}|} \qquad (10)$$

and the sense of the angle by the vector cross product.

ii) The aligned lattice rows must have the same spacing. As $\mathbf{q}_{hk} = \mathbf{q}^{pq}$ it follows that

$$\lambda_{hk} = \lambda^{pq} \qquad (11)$$

(This requirement is the analog of the Bragg condition of crystallography)

When the spacing is dissimilar, the misfit may be accommodated in several ways. If the crystal strains homogeneously, increasing strain energy but decreasing misfit energy, (as in the case of pseudomorphic growth), the matching may be one-dimensional, (atomic spacing along the rows is still unequal) or two-dimensional when both the perpendicular row spacing

as governed by conditions (7)and (11) and the atom positions along the rows match. Two-dimensional coherency, requires that the epitaxial criterion is satisfied by *two non-colinear pairs* of substrate and overgrowth reciprocal lattice vectors[18,19].

Alternatively, misfit dislocations may be introduced to accommodate both orientational and dimensional mismatch by screw and edge misfit dislocation arrays respectively[22,30-34].

QUALITY FACTORS DERIVED FROM THE MODEL

The requirement of the energy inequality (1) of minimizing the interfacial energy γ_I results in several quality factors which allow selection between several possible configurations which satisfy the epitaxial criterion (eq 7).

Factor 1: *Epitaxial Strength*

When a particular substrate wave vector $\mathbf{q}_{hk}$ resonates with the overgrowth vector $\mathbf{q}^{pq}$, the contribution to the misfit energy is positive or negative depending on the sign of V_{hk} and of the product of sine-expressions. Additionally the total reduction in misfit energy achieved by a particular system is given by the sum of all the V_{hk} terms (with signs) which resonate in this fashion. This sum of Fourier coefficients active in a particular epitaxial orientation is a measure of the tendency to epitaxy[18], and has been termed the *epitaxial strength*. Hence, the epitaxial strength is defined by

$$\textit{Epitaxial Strength} \equiv \sum_{\substack{h,k \\ (h,k)\neq(0,0) \\ p,q\ \textit{integer}}} V_{hk}\,\mathrm{sgn}\left(\frac{\sin \pi(2M+1)p(h,k)}{\sin \pi p(h,k)} \cdot \frac{\sin \pi(2N+1)q(h,k)}{\sin \pi q(h,k)}\right) \qquad (12)$$

where sgn refers to the sign of the expression between brackets, and the sum is taken only over those h, k which satisfy the epitaxial criterion in the given configuration. Clearly, configurations with *large negative* values of epitaxial strength are preferred.

Factor 2: ***Relative density of coinciding reciprocal lattice points***

A geometric consequence is a weaker form of the same condition, namely the configuration which has more coinciding reciprocal lattice vectors is preferred, as then the summation is taken over more terms. A quality factor then is the *relative density of coinciding reciprocal lattice points*. The higher the coincidence of reciprocal lattice points, the better.

Factor 3: ***Order of the Fourier term, length of the reciprocal lattice vectors***

It has been shown by Stoop[35] in model studies using atomistic potentials that the magnitude of Fourier coefficients tends to decrease rapidly with order (|h|+|k|, |p|+|q|). A consequence is that the contribution to the epitaxial strength, and interfacial energy reduction, is such that the shorter the reciprocal lattice vectors which resonate, (as seen in reciprocal space) the likelier will be the actual occurrence of the particular epitaxial configuration.

Factor 4: ***Strain energy density***

Real systems might be expected to strain to achieve pseudomorphic structures, depending on the gain in misfit energy compared to the cost in strain energy, both of which contribute to the interfacial energy density, γ_I. The strains may be calculated directly from the reciprocal lattice, and a measure of the strain energy is provided by the strain energy density calculated from the strains and known plane stress elastic constants (suitable for thin films) calculated for the overgrowth orientation. Configurations with lower *strain energy density* are preferred.

Of these quality factors, the latter three are essentially geometric in nature, and will be used to order possible epitaxial configurations.

SPECIAL CONSIDERATIONS IN COVALENT POLYATOMIC SYSTEMS

The expression (2) is given in its simplest from, and to be useful for systems of several atom types, or bonding states, a Fourier series for each atom type represented in the overgrowth for V_a, and similarly, for each substrate species a series for V_b, and cross interactions, should be constructed. However all lead to the same epitaxial criterion, although partial or complete extinction of some reciprocal lattice points is possible, which results in the introduction of structure factors to each coefficient. Localization of the bond in the unit cell to model covalent bond directionality may be achieved by careful choice of Fourier coefficients, in particular some higher order terms are not independent of low order terms[18].

APPLICATION TO THE DIAMOND - BN_{cub} SYSTEM

In order to apply the epitaxial criterion it is necessary to construct the reciprocal spaces of both the overgrowth and substrate surface lattices. We have generally chosen primitive surface lattices to avoid complications with structure factors due to non-primitive unit cell constructions. Needed are surface unit cell parameters (angles and lengths obtainable from Table I) and the relative lattice scaling parameter, usefully given as the ratio of nearest neighbour distances in the bulk (eq 6b), which was chosen as $r = 0.986489$ for this study.

Two-dimensional plane stress elastic constants suitable to the overgrowth orientation are required when strain energy densities and the strains of one-dimensional matching conditions are calculated. These boundary conditions require the upper surface of the overgrowth to be free of stresses in the normal direction, $\sigma_{zi} = \sigma_{iz} = 0$, i= x, y, z and stresses independent of z.

We have used the program LATUSE/SARCH by van Hove and Hermann[36] to determine the surface cell structures, and our own program ELCON to transform elastic constants to the

required plane and apply the plane stress boundary conditions. The reciprocal space searches were carried out with an interactive version of the program ORPHEUS[18]. Both programs ELCON and ORPHEUS are available for MSDOS and Apple Macintosh computers.

The ORPHEUS program produces scaled plots of the substrate and overgrowth reciprocal lattices and interactively leads the user through a construction analogous to the Ewald construction of crystallography. By selecting a substrate reciprocal vector, $\mathbf{q}_{hk}$, and drawing a circle, centered at the origin, through its end, the locus of the end-point of the vector as it is rotated through 360° is constructed. Any overgrowth reciprocal lattice point which lies on this circle describes an overgrowth reciprocal lattice translation vector, $\mathbf{q}^{pq}$ equal in length to $\mathbf{q}_{hk}$. The angle between $\mathbf{q}^{pq}$ and $\mathbf{q}_{hk}$ determines the orientation angle, this being the angle θ_R through which the overgrowth must be rotated to come into epitaxial orientation with the substrate. The strains needed to bring a vector nearly on the circle into coincidence and the associated energy are calculated from the components of the selected vectors. The selection of substrate and overgrowth vectors, and the subsequent calculation of angles of rotation, strains and strain energies are done interactively with the ORPHEUS program. Plots showing the subsequent reciprocal lattices in coincidence are produced by the program, from which quality judgements of the density of points which coincide may be made.

As both Diamond and BN_{cub} share the geometry of the zincblende structure a single set of unit cell descriptions is given for the planes which were considered.

The results are summarized in Table II, where the matching conditions which give lowest strain energy in several plane combinations are given. For like planes an isotropic extensive strain of 1.37% introduces two-dimensional pseudomorphy "P" with zero misfit energy and a strain energy density of 2.2×10^9erg cm^{-3} , only twice as high as the one-dimensional matching case, "P^1" (typically, 1.09×10^9erg cm^{-3}), which has an increased misfit energy.

Several partially matching cases are distinguished in Table II, and these form a hierarchy ordered by the density of reciprocal lattice points that are paired in both overgrowth and substrate. Of lowest misfit energy is the 2-dimensional pseudomorphic case, in which there is perfect continuation of the substrate lattice into the overgrowth. This occurs only for like planes. The Diamond{100} on BN_{cub}{100) case is presented as an illustration in Fig. 1. A less favorable case is indicated by "P^{-2}", in which all overgrowth reciprocal lattice vectors match substrate vectors, but some substrate vectors do not have counterparts in the overgrowth reciprocal lattice. This occurs only in the epitaxial configuration in which Diamond{100} grows on BN_{cub}{221}, as shown in Fig. 2. The cases indicated by "(2)" in the table have coincidence matching in at least one direction, where some overgrowth reciprocal lattice vectors do not have matched counterparts in the substrate, and some substrate points do not have counterparts in the overgrowth. An example is presented in Fig. 3.

A similar hierarchy of one dimensional matching cases is also distinguished in Table II by the superscript "^{1}" in the "Type" column.

Of most interest is the Diamond{100} matching with the BN_{cub}{221} . Here isotropic strain of 1.37% introduces two-dimensional coincidence, but with irregular matching in the Diamond[0 1 $\bar{1}$] direction when parallel with the BN_{cub}[1 1 $\bar{4}$] direction. These are the same strains as for the pseudomorphic Diamond{100} // BN_{cub}{100} case. No other low-index plane combination of unlike planes yielded 2-dimensional coherency of this quality.

The results may be summarized as showing that the two-dimensional pseudomorphic matching (Fig. 1) is only a little more expensive in strain energy than one-dimensional pseudomorphy in like planes, but is expected to produce considerable savings in misfit energy. The second best matching possibility is the Diamond{100} on BN_{cub}{221} case

(Fig.2), identical in strain energy to pseudomorphic cases, but with increased misfit energy, due to coincidence matching and correspondingly poorer epitaxial strength. Although other unlike diamond planes could achieve one dimensional or coincidence matching, within the same low strain energy, they are not expected to compete with these low-order candidates because of their still higher misfit energy and hence poorer epitaxial strength. Of other unlike pairs, the Diamond{100} on BN_{cub}{112} configuration (Fig. 3) has a two dimensional configuration with a strain energy density of 1.35×10^9erg cm^{-3} comparable to the one dimensional case. However, this is only a rather high order coincidence match in which every fifth substrate reciprocal lattice point coincides with every second overgrowth point resulting in an increased misfit energy contribution from surface energy mismatch. The configuration is possibly better than one dimensional matching, but somewhat unfavourable when compared to the possibility of pseudomorphic Diamond{112} on BN_{cub}{112}. Other unlike planes do not have the possibility of two dimensional coherency within such a low energy so making it unlikely that other unlike planes will grow epitaxially.

The experiments reported by Koizumi *et al* [14], Yoshikawa *et al*[15] and Murakami *et al*[16] indicate results which agree well with the geometric considerations presented here. In the low-index substrates diamond prefers to grow in pseudomorphic arrangement to the alternative but higher index coincidence planes. In the BN_{cub}{221} case Diamond apparently grew in a low-index {100} orientation in preference to a pseudomorphic {221} configuration.

From the present theoretical results this would be expected since there is essentially no difference in strain energy between the {221} on {221} and {100} on {221} configurations. Thus, which configuration actually occurs, is expected to be determined by the surface energy differences of the growth islands and by kinetic factors such as growth rates of the different directions and planes. This in turn will be influenced by such factors as supersaturation and impurities present during growth which are dependent on the specific growth system and

growth parameters employed. It should be noted that, unfortunately, complete experimental confirmation of {100} growth of Diamond on the {221} BN_{cub} face has not been established since the exact nature of the interface has not yet been determined due to the limited size of the BN_{cub} substrates (on the order of 100 μm).

The Diamond{100} on BN_{cub}{112} configuration has not yet been examined experimentally, and the question is raised whether diamond would tolerate epitaxial configurations only as far as the {100} on {221} P^{-2} case. If so, this could be used as a threshold from which the importance of the quality factors can be deduced. It should also be noted that a reduced surface energy mismatch might allow further progression down the hierarchy of configurations to one dimensional matching or other two dimensionally coincident cases with low strain energy density.

CONCLUSION

The Diamond-BN_{cub} system appears to agree with the geometric considerations as expressed in the reciprocal lattice criterion. This does show the potential of addressing not only surface energies when considering candidate systems for epitaxial growth, but of also addressing minimization of interfacial energy within a straightforward geometric technique.

Low index like planes have been observed to grow pseudomorphically experimentally, and the geometrically derived low required strain of 1.37% from bulk parameters is consistent. The unlike epitaxial configuration which pairs Diamond{100} with BN_{cub}{221} yields two-dimensional coincidence with the same small strain, and is favoured above other low-index mixed configurations in this way. The reason for observed {100} growth as opposed to {221} growth of the diamond is probably due to surface energy properties and conditions during growth, although as was pointed out, the experiment itself is ambiguous about the possibility

that the {221} orientation is actually retained in the interface, transforming into a {100} orientation some distance away from the interface.

The rigidity of diamond suggests that geometric criteria are particularly suitable as a tool for selecting candidate substrate planes, particularly important where structures of dissimilar types are considered as substrate candidates. The reciprocal lattice provides clarity where considerations with atomic rows tend to be clouded by details of atomic positions.

Candidate surfaces of other and dissimilar structures will be sought with these techniques.

ACKNOWLEDGEMENTS

This work was supported in part by grants from SDIO/IST through ONR and the Office of Naval Research itself. One of us (MWHB) is currently on sabbatical leave from the University of Pretoria and acknowledges the grant of leave and the financial burden carried by CEFIM at that university.

REFERENCES AND FOOTNOTES

1 Permanent Address: Department of Physics, University of Pretoria, Pretoria, South Africa

2 Landolt-Börnstein Tables, "Numerical Data and Functional Relationships in Science and Technology", New Series **III/17d**, "Technology of III-V, II-VI and Non-Tetrahedrally Bonded Compounds", Springer Verlag, Berlin (1987)

3 J.E. Field "Properties of Diamond", (Academic Press, London, 1979)

4 V.K. Bazhenov, I.M. Vikulin and A.G. Gontar, Sov. Phys. Semicond. **19**, 829, (1985)

5 B. Singh, Y. Arie, A.W. Levine and O.R. Mesker, Appl. Phys. Lett. **52**, 451, (1988)

6 S. Matsumoto and Y. Matsui, J. Mater. Sci. **18**, 1785, (1983)

7 A. Sawabe and T. Inuzuka , Thin Solid Films **137**, 89, (1986)

8 S. Matsumoto, J. Mater. Sci. Lett., **4**, 600, (1985)

9 Y. Sato, M. Kamo and N. Setaka in "High Tech Ceramics", edited by P Vincenzini, (Elsevier Science Publishers, BV, Amsterdam, 1987)

10 B.V. Derjaguin, B.V. Spitsyn, A.E. Gorodetsky, A.P. Zakharov, L.I. Bouilov and A.E. Aleksenko, J. Cryst. Growth, **31**, 44, (1975)

11 Derjaguin, BV, Fedoseev, DV; Polyanskaya, ND; Statenkova, EV; Sov Phys Crystallogr, **21**, (1976), 239

12 Geis, MW; presented at the Third Annual SDIO-IST/ONR Diamond Technology Initiative Symposium, Crystal City, VA, 1988

13 Nakazawa, H; Kanazawa, Y; Kamo, M; Osumi, K; Thin Solid Films, **151**, (1987), 451

14 Koizumi, S; Murakami, T; Inuzuka, T; Suzuki, K
"Epitaxial Growth of diamond thin films on cubic boron nitride {111} surfaces by DC plasma chemical vapour deposition."
[Submitted to Appl Phys Lett. (May 30 1990)]

15 Yoshikawa, M; Ishida, H; Ishitani, A; Murakami, T; Koizumi, S; Inizuka, T;
"Study of crystallographic orientations in the diamond film on c-BN using Raman Microprobe"
[Submitted to Appl Phys Lett. (May 30 1990)]

16 Murakami, T; Koizumi, S; Suzuki, K; Inuzuka, T; "Epitaxial growth of diamond on high pressure synthesized c-BN particles", presented at the fall meeting of the Japan Society of Applied Physics, Fukuoka, Japan, September 27-28, 1989

17 Fletcher, NH; Lodge, KW; in "Epitaxial Growth, Part B", JW Matthews ed, Academic Press, New York, (1975) 529

18 Braun, MWH; "Epitaxy on substrates with hexagonal lattice symmetry" DSc Thesis, University of Pretoria Nov 1987

19 Braun, MWH; van der Merwe, JH; South African J of Science **84** (1988) 670

20 van der Merwe, JH; Phil Mag **45**, (1982) 127, 145, 159

21 Reiss, H; J Appl Phys **39**, (1968) 5045

22 Frank, FC; van der Merwe, JH; Proc Roy Soc, **A 198**, (1949) 205, 216; **A 200**, (1950) 125, 261

23 van der Merwe, JH; Proc Phys Soc, (London), **A 63**, (1950) 616, 1370

24 Gotoh, Y; Arai, I; Japan J Appl Phys, **25**, (1986) L583

25 Bauer, E; Z Kristallogr, **110**, (1958), 372

26 van der Merwe, JH; Bauer, E; Phys Rev B, **39**, (1989), 3632

27 Busch, G; Schade, H; "Lectures on Solid State Physics", Ferdinand Cap transl, Pergamon Press, Oxford (1976) , 16

28 Kittel, C; "Introduction to Solid State Physics", John Wiley and Sons, New York, 4 ed, (1971), 43

29 Bruce, LA; Jaeger, H; Phil Mag, **36**, (1977) 1331; **37**, (1978) 337; **38**, (1978) 223

30 van der Merwe, JH; Proc Phys Soc (London), A **63**, (1950), 616, 1370

31 Matthews, JW; in "Epitaxial Growth, Part B", JW Matthews ed, Academic Press, New York, (1975), 559

32 Jesser, WA; Phys Stat Solidi a, **20**, (1973), 63

33 Jesser, WA; Kuhlmann-Wilsdorf, D; Phys Stat Solidi, **19**, (1967), 95; **21**, (1967), 533

34 Kishino, S; Ogirima, M; Phil Mag, **31**, (1975), 1239

35 Stoop, PM; Snyman, JA; Thin Solid Films, **163**, 503

36 van Hove, MA; Hermann, K; LATUSE and SARCH, Univ of California, Berkeley, Ca 94720, USA

Table I: This Table shows the unit cell choices for several low-index planes in the underlying structure of both Diamond and BN_{cub}. Lattice Parameters are 3.56685Å and 3.6157Å for Diamond and BN_{cub} respively.[a]

h k l	$\mathbf{a}_1$ or $\mathbf{b}_1$	$\mathbf{a}_2$ or $\mathbf{b}_2$	α or β
1 0 0			
$\frac{1}{2}[0\ \bar{1}\ \bar{1}]$	$\frac{1}{2}[0\ 1\ \bar{1}]$	90	
1 1 0	$\frac{1}{2}[1\ \bar{1}\ 0]$	$[0\ 0\ \bar{1}]$	90
1 1 1	$\frac{1}{2}[1\ \bar{1}\ 0]$	$\frac{1}{2}[1\ 0\ \bar{1}]$	60
1 2 0	$[0\ 0\ \bar{1}]$	$\frac{1}{2}[\bar{2}\ 1\ \bar{1}]$	65.9
1 1 2	$\frac{1}{2}[1\ \bar{1}\ 0]$	$[1\ 1\ \bar{1}]$	90
1 1 4	$\frac{1}{2}[1\ \bar{1}\ 0]$	$[2\ 2\ \bar{1}]$	90
2 2 1	$\frac{1}{2}[1\ \bar{1}\ 0]$	$\frac{1}{2}[1\ 1\ \bar{4}]$	90

a Landolt-Börnstein Tables, "Numerical Data and Functional Relationships in Science and Technology", New Series **III/17d**, "Technology of III-V, II-VI and Non-Tetrahedrally Bonded Compounds", Springer Verlag, Berlin (1987)

Table II: Epitaxial orientations for varous combinations of dissimilar planes in which the geometric relationship which minimizes strain energy are shown for low-index planes. Diamond forms the overgrowth in all cases.

Planes: BN_{cub} Diamond		Lattice Directions: Parallel rows (S: Secondary - Note 1) (B: Boron Nitride, C:Diamond)		Zero Misfit Direction	Strains (ε_x ε_y) (ε_x ε_y γ_{xy} if $\gamma_{xy}\neq 0$) (Note 2)	Strain Energy density ($\times 10^9$ erg cm^{-3})	Type (Note 3)
Like Planes:							
h k l	h k l	B	[u v w]	[U V W]	1.37%	1.09†	P[1]
		C	[u v w]	[U V W]	-0.01%		
†This energy may vary by about 10% due to anisotropy in high order planes.							
		S: B	[U V W]	[u v w]	1.37%	2.20	P
		S: C	[U V W]	[u v w]	1.37%		
Unlike Planes:							
2 2 1	1 0 0	B	[$\bar{1}$ $\bar{1}$ 4]	[1 $\bar{1}$ 0]	1.37%	1.09	P[1]
		C	[0 $\bar{1}$ 1]	[0 $\bar{1}$ $\bar{1}$]	-0.01%		
		S: B	[1 $\bar{1}$ 0]	[$\bar{1}$ $\bar{1}$ 4]	1.37%	2.20	P-2
		S: C	[0 $\bar{1}$ $\bar{1}$]	[0 $\bar{1}$ 1]	1.37%		
	1 1 0	B	[$\bar{1}$ $\bar{1}$ 4]	[1 $\bar{1}$ 0]	1.37%	1.09	P[1]
		C	[0 0 1]	[1 $\bar{1}$ 0]	-0.16%		
	1 1 0	B	[1 $\bar{3}$ 4]	[11 $\bar{7}$ $\bar{8}$]	2.15%	6.57	P[1]
		C	[1 $\bar{1}$ 2]	[1 $\bar{1}$ $\bar{1}$]	1.00% 3.25%		
	1 1 1	B	[$\bar{1}$ $\bar{1}$ 4]	[1 $\bar{1}$ 0]	1.37%	1.09	P-1
		C	[$\bar{1}$ $\bar{1}$ 2]	[1 $\bar{1}$ 0]	-0.11%		
		S: B	[1 $\bar{3}$ 4]	[11 $\bar{7}$ $\bar{8}$]	-12.2%	86.8	(2)
		S: C	[0 $\bar{1}$ 1]	[2 $\bar{1}$ $\bar{1}$]	1.37%		

Table II: (Cont):
Epitaxial orientations for varous combinations of dissimilar planes in which the geometric relationship which minimizes strain energy are shown for low-index planes. Diamond forms the overgrowth in all cases.

Planes: BN_{cub}	Diamond		Lattice Directions: Parallel rows (S: Secondary - *Note 1*) (B: Boron Nitride, C:Diamond)	Zero Misfit Direction	Strains (ε_x ε_y) (ε_x ε_y γ_{xy} if $\gamma_{xy}\neq 0$) *(Note 2)*	Strain Energy density ($\times 10^9$ erg cm^{-3})	Type *(Note 3)*
2 2 1	1 1 2	B	$[\bar{1}\ \bar{1}\ 4]$	$[1\ \bar{1}\ 0]$	1.37%	1.13	P1
		C	$[\bar{1}\ \bar{1}\ 1]$	$[1\ \bar{1}\ 0]$	-0.06%		
		S: B	$[1\ \bar{3}\ 0]$	$[1\ 1\ \bar{4}]$	1.37%	1.35	(2)
		S: C	$[1\ \bar{1}\ 0]$	$[1\ 1\ \bar{1}]$	-0.68%		
	1 1 2	B	$[1\ \bar{1}\ 0]$	$[1\ 1\ \bar{4}]$	1.37%	1.13	(1)
		C	$[\bar{1}\ \bar{1}\ 1]$	$[1\ \bar{1}\ 0]$	-0.06%		
	1 1 4	B	$[\bar{1}\ \bar{1}\ 4]$	$[1\ \bar{1}\ 0]$	1.37%	1.09	P1
		C	$[2\ 2\ \bar{1}]$	$[1\ \bar{1}\ 0]$	-0.02%		
	1 1 4	B	$[1\ \bar{1}\ 0]$	$[1\ 1\ \bar{4}]$	1.37%	1.09	(1)
		C	$[2\ 2\ \bar{1}]$	$[1\ \bar{1}\ 0]$	-0.02%		
	1 2 0	B	$[1\ \bar{3}\ 4]$	$[11\ \bar{7}\ \bar{8}]$	-0.06%	0.024	P1
		C	$[2\ \bar{1}\ \bar{3}]$	$[6\ \bar{3}\ \bar{5}]$	-0.13% -0.20%		
		S: B	$[3\ \bar{2}\ \bar{2}]$	$[\bar{2}\ 7\ \overline{10}]$	-2.86%	4.94	(2)
		S: C	$[\bar{2}\ 1\ \bar{2}]$	$[\bar{4}\ 2\ \bar{5}]$	1.37%		

Table II: (Cont):
Epitaxial orientations for varous combinations of dissimilar planes in which the geometric relationship which minimizes strain energy are shown for low-index planes. Diamond forms the overgrowth in all cases.

Planes: BN_{cub}	Diamond		Lattice Directions: Parallel rows	Zero Misfit Direction	Strains (ε_x ε_y) (ε_x ε_y γ_{xy} if $\gamma_{xy}\neq 0$) *(Note 2)*	Strain Energy density ($\times 10^9$ erg cm^{-3})	Type *(Note 3)*
		(S: Secondary - *Note 1*) (B: Boron Nitride, C:Diamond)					
1 1 0	1 0 0	B	[0 0 1]	[1 $\bar{1}$ 0]	1.37%	1.09	P[1]
		C	[0 $\bar{1}$ 1]	[0 $\bar{1}$ $\bar{1}$]	-0.01%		
		S: B	[1 $\bar{1}$ 0]	[0 0 $\bar{6}$]	1.37%	12.4	(2)
		S: C	[0 $\bar{1}$ $\bar{1}$]	[0 1 $\bar{1}$]	-4.4%		
1 2 0	1 1 0	B	[0 0 $\bar{1}$]	[$\bar{2}$ 1 0]	-1.21%	2.06	P[1]
		C	[1 $\bar{1}$ 2]	[1 $\bar{1}$ $\bar{1}$]	-0.56% -1.82%		
	1 1 0	B	[2 $\bar{1}$ 0]	[0 0 $\bar{1}$]	-0.14%	0.99	(1)
		C	[1 $\bar{1}$ 0]	[0 0 $\bar{1}$]	1.37%		
		S: B	[2 $\bar{1}$ $\bar{3}$]	[$\bar{6}$ 3 5]	6.85%	29.8	(2)
		S: C	[1 $\bar{1}$ $\bar{2}$]	[$\bar{1}$ 1 $\bar{1}$]	1.37%		
1 1 2	1 0 0	B	[$\bar{1}$ $\bar{1}$ 1]	[1 $\bar{1}$ 0]	1.37%	1.09	P[1]
		C	[0 $\bar{1}$ 1]	[0 $\bar{1}$ $\bar{1}$]	-0.01%		
		S: B	[1 $\bar{1}$ 0]	[1 1 $\bar{1}$]	1.37%	1.35	(2)
		S: C	[0 $\bar{1}$ $\bar{1}$]	[0 1 $\bar{1}$]	-0.68%		
1 1 2	1 1 0	Nothing within a strain of 4%					
1 1 2	1 1 1	Nothing within a strain of 8%					

Notes on Table II:

1. Secondary matching conditions (S) refer to directions in the overgrowth and substrate which match in addition to those which already resulted in the one-dimensional coherency. These increase the type of matching to two-dimensional when the new strains are applied.

2. The cartesian coordinates in which strains are expressed are chosen with the x-direction parallel to the unit cell vector $\mathbf{b}_1$ and the z-direction perpendicular to the plane. Additionally, the y-direction is perpendicular to both, and the vectors form a right-handed system.

3 Types of matching are identified as follows:
2-dimensional match:

P: exact continuation of the substrate structure, including interfacial lattice parameters, as Pseudomorphic (P). (Applies to both reciprocal and direct spaces)

P^{-2}: all overgrowth reciprocal lattice points match exactly to substrate points, but some substrate points do not have overgrowth counterparts

(2): refers to the general case of two-dimensional coherency with coincidence in either the Frank or Bollmann senses, but excludes the pseudomorphic case. 1-dimensional pseudomorphism, in the P^1-sense may still be present.

1-dimensional match:

P^1: exact matching of all reciprocal lattice points of the overgrowth with all of those of the substrate in one direction in reciprocal space. Direct space lattice rows are equally spaced and parallel, but lattice positions along the rows are not in coincidence.

P^{-1}: all overgrowth reciprocal lattice points coincide with substrate points, but not all substrate points have counterparts in the overgrowth, one-dimensionally.

(1): some overgrowth and substrate points fail to match, while overgrowth reciprocal lattice points periodically match substrate popints. Coincidence in the Frank or Bollmann senses occurs, but one-dimensionally.

FIGURE CAPTIONS

Figure 1: Superimposed reciprocal spaces of the Diamond and cubic Boron Nitride {100} faces showing full pseudomorphism (P in Table II) after isotropic strain of 1.37%.
The symbols : ◉ indicate matched overgrowth and substrate points

Figure 2: Superimposed reciprocal lattices of the Diamond {100} and cubic Boron Nitride {221} surfaces, showing the coincidence matching after isotropic 1.37% strain. This matching configuration is referred to as P^{-2} in the Table II and in the text.
The symbols : ◉ indicate matched overgrowth and substrate points, ● mean substrate reciprocal lattice points which do not have partners in the overgrowth.

Figure 3: Superimposed reciprocal lattices of the Diamond {100} and cubic Boron Nitride {112} surfaces, showing the coincidence matching after strain of $\varepsilon_{xx} = 1.37\%$, $\varepsilon_{yy} = -0.68\%$. This matching configuration is an example of the type (2) in the Table II and in the text.
The symbols : ◉ indicate matched overgrowth and substrate points, ● mean substrate reciprocal lattice points which do not have partners in the overgrowth, ⊙ mean overgrowth points which do not have partners in the substrate.

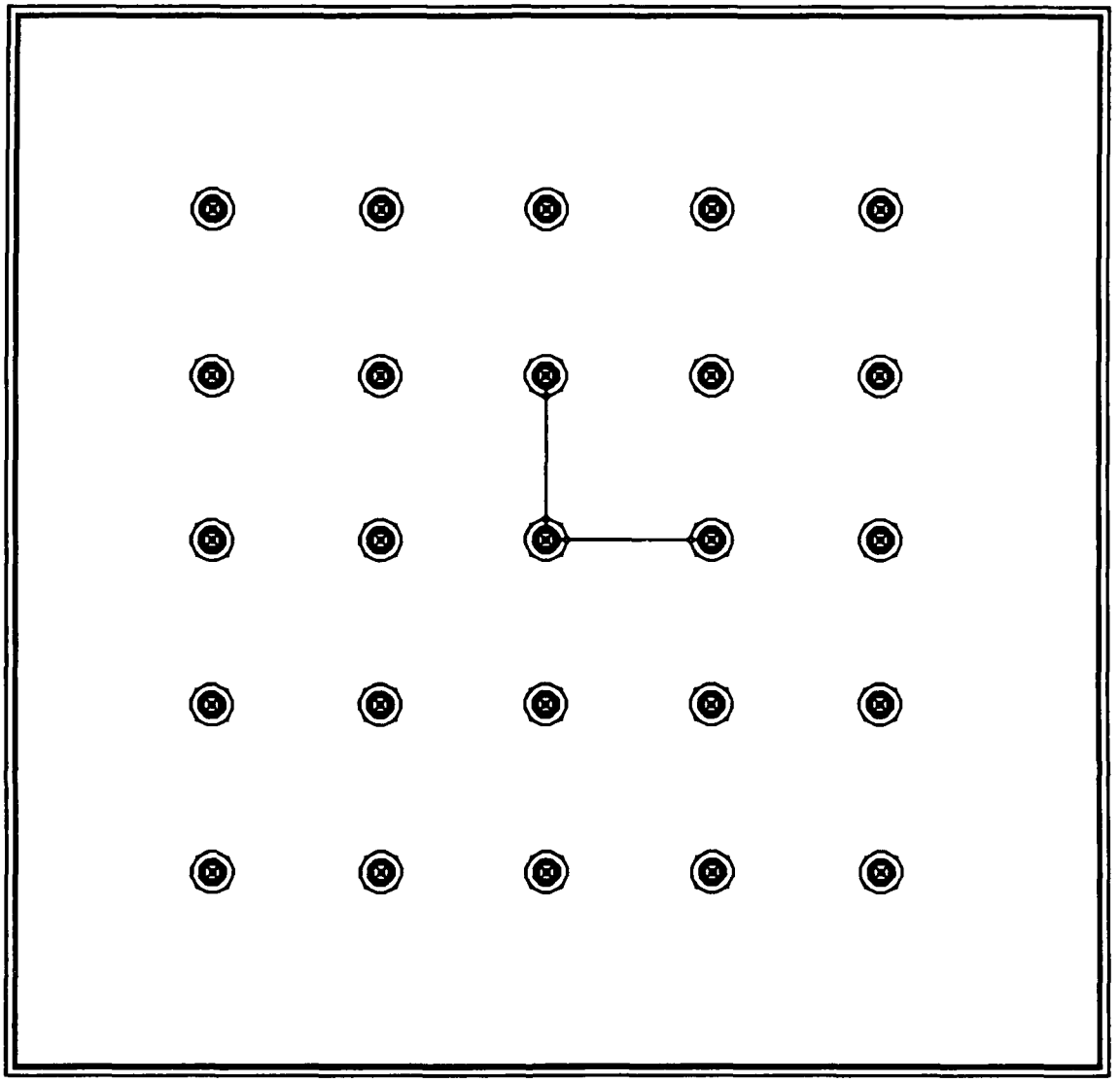

Figure 1: MWH Braun[1] , HS Kong, JT Glass and RF Davis,: Journal of Applied Physics

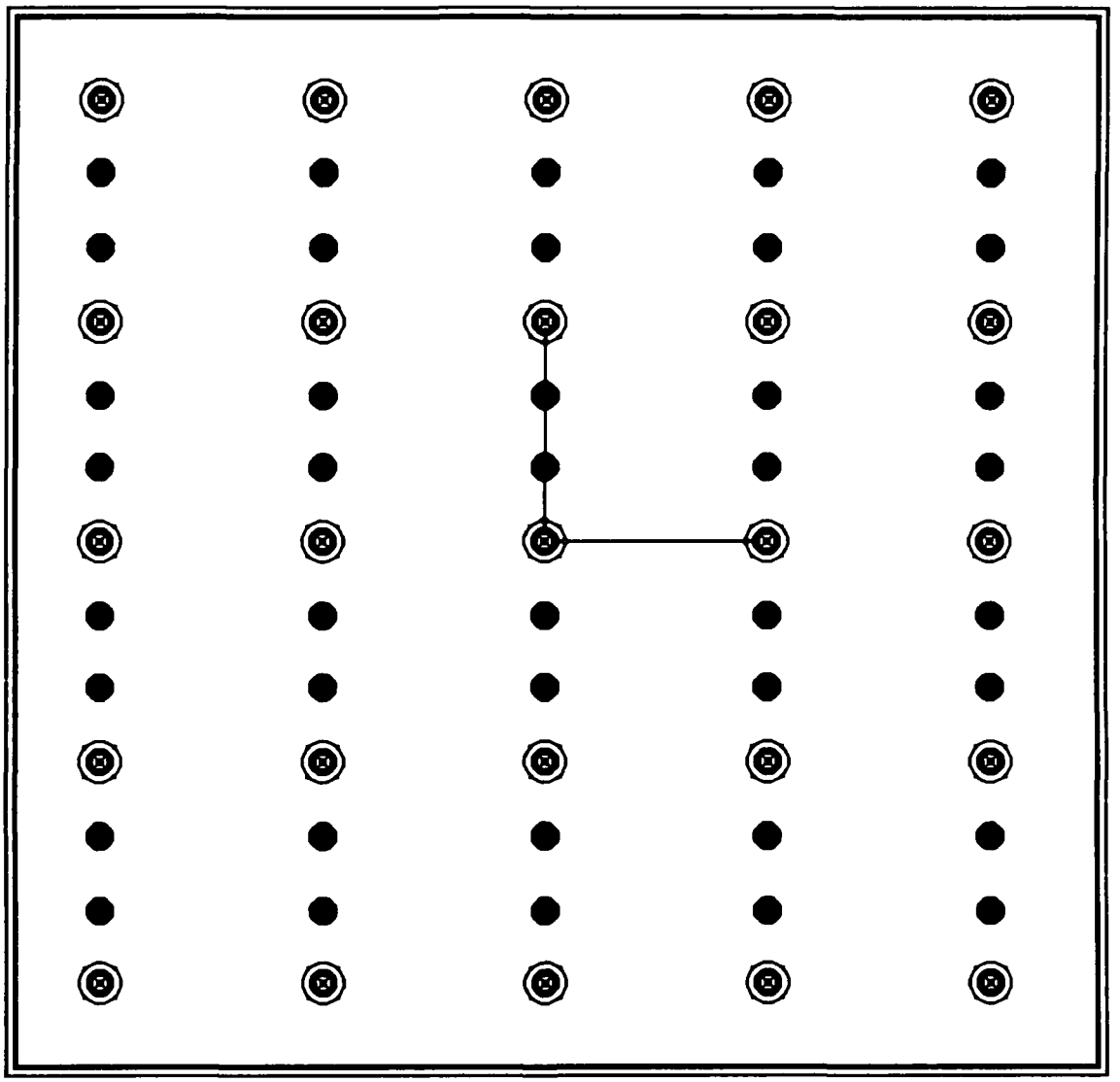

Figure 2:.MWH Braun[1] , HS Kong, JT Glass and RF Davis,: Journal of Applied Physics

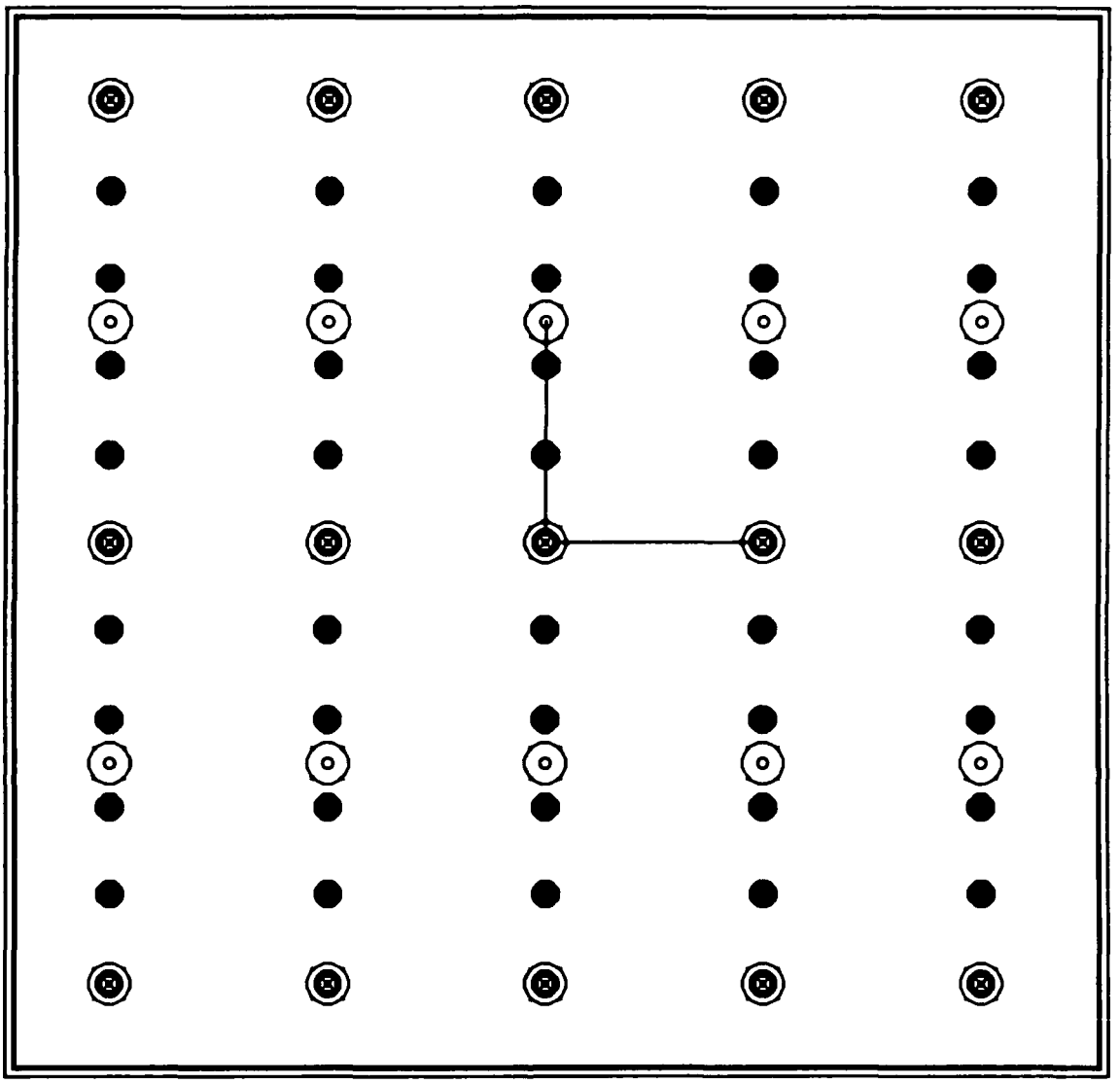

Figure 3:.MWH Braun[1] , HS Kong, JT Glass and RF Davis,: Journal of Applied Physics

Novel Approaches to the Attainment of the Heteroepitaxy of Diamond Films

Anand Vasudev and Dr. Robert F. Davis
Department of Materials Science and Engineering
North Carolina State University

Introduction

Attempts to grow diamond films on other single crystal substrates, such as Ni, cBN, or SiC have been unsuccessful due to the difficulty in nucleating diamond on a foreign substrate. However, these attempts at heteroepitaxy of diamond have primarily dealt with the conventional vapor transport processes, such as plasma assisted chemical vapor deposition (CVD).

The goal of this study is to achieve epitaxial growth of single crystal diamond films on one or more nondiamond substrates. The resulting film can be extremely thin - e.g., 50 - 500Å; since, it will be used as the substrate on which to grow thicker diamond films by a more conventional process such as plasma CVD. The techniques given below may be divided into three groups: (a) high pressure, (b) ion beam enhanced epitaxy, and (c) the use of surfactants.

A. The Use of the Pressure Variable for the Conversion of Amorphous "Diamond"

The objective of this approach is to form monocrystalline diamond films by producing thin, H-free diamond-like C films on suitable substrates followed by exposure of the assemblies to sufficient pressure and temperature to cause crystallization to diamond. The reasoning which supports this approach follows both from the enhanced crystallization and diffusion rates produced by the negative (assumed) activation volume and the driving force of epitaxial relationships. It may be necessary (or at least helpful) to use epitaxy to cause the formation of diamond, if we can get the film to crystallize from the substrate to the film surface rather than vice-versa which is the more common case. The initial substrates will be Diamond(110), Si(100) and ß-SiC(100). The biggest concern of ours in conducting this study is to be able to apply pressure to the diamond-like amorphous C film and to simultaneously monitor any structural changes in the film, especially the nature of the bonding.

Dr. David Schefferal of Los Alamos National Laboratory who has a high-pressure diamond anvil cell that is capable of doing in-situ Raman spectroscopy will collaborate with us. Raman Spectroscopy will tell us the nature of the films in terms of its amorphous nature and the mixture of sp^2 and sp^3 bonding. Since the pressure cell contains diamond the laser beam for the Raman analysis will have to be focused such that only the film is being analyzed. This is made possible by a technique called Confocal Micro-Raman Spectroscopy, which incorporates an additional lens into the optics to focus the laser beam into a finer focal point. The pressure is measured using a very small ruby crystal that is placed near the sample. Fortunately, we have a similar but lower temperature and pressure apparatus in the physics department at NCSU which is under the supervision of Dr. Michael Paesler. Dr. Paesler and his student (Gerd Pheiffer) have agreed to assist us in the preparation of the samples.

The upper limits of the high-pressure diamond anvil cell at Los Alamos are as follows:

Maximum Pressure = 200 kbar

Maximum Temperature = 900°C (long term use @ 700°C)

Maximum sample dimensions = 0.1mm X 0.1mm X 0.1mm

Pressure medium = cryogenic Argon.

Cryogenic Argon (80K) is used as a pressure medium to insure that the applied pressure is homogeneously distributed across the surface.

H-free amorphous carbon films are desired because, if present, H ties up dangling C bonds which would preferrably become sp^3 under selected pressure/temperature regimes. A method called Elastic Recoil Detection (ERD) will be used to measure the H content in the diamond-like C films. (This method is described in more detail by: H.C. Hofsass, et al, Nuclear Instruments and Methods in Physics Research B45, pp. 151-156 (1990)). ERD is a highly sensitive technique for detecting light elements in thin samples containing heavier elements. In this technique MeV He^+ ions are incident on a thin target and the energies of both the forward-scattered He ions and the elastically recoiled light atoms are detected in coincidence. Concentration-versus-depth profiles can be obtained from the measured number of coincidence events for a depth range of 1μm and for all recoiled light elements.

Dr. Bruce Sartwell at the Naval Research Laboratory in Washington D.C. will characterize the diamond-like C films for H content using ERD. The amount of sp^3 bonding in the film also needs to be determined prior to the application of pressure. Dr. James E. Butler at the Naval Research Laboratory, Chemistry Division will analyze the bonding nature of the film using Raman Spectroscopy .

B. Ion Beam Enhanced Epitaxy (IBEE) of Diamond and Amorphous-C Films

In this study a (100) diamond crystal will be ion implanted (@ 77K) using a C ion beam and sufficient energy and dosage to amorphize the surface layer. The tempreature and energy of the second C implant will be raised to cause solid phase epitaxy (SPE) of the amorphized layer. The thickness of the amorphized layer must be thin in order to achieve epitaxy completely to the surface. The beauty of this technique is that the recrystallization begins at the substrate/amorphized layer interface rather than at the surface.

Alternatively, an amorphous carbon film will be deposited on (100) diamond and on other substrates such as (100) and (0001) SiC, polycrystalline cBN and (100) Ni. Subsequently, high energy C ion implantation will be conducted to cause SPE on the selected substrates. Dr. Stephen Withrow of Oak Ridge National Laboratories in Knoxville, Tennessee has agreed to work with us on the ion implantation of the samples. The parameters which influence the regrowth rate, such as

dose rate, target, target temperature, ion species, and ion energies will have to be optimized. Listed below are preliminary estimates for these parameters:

Targets	Ion Species	Temperature	Energies(keV)	Dose Rate(ions/cm^2)
(100) Diamond	C	77K	150-225	1.5 - 5.0 x 10^{15}
Amorphous Diamond	C	300-500°C	250-350	10^{16} - 10^{17}
Amorphous C	C	300-500°C	250-350	10^{16} - 10^{17}

C. The Use of Surfactants to alter the Surface Energies of the Substrate and Diamond Film

The combination of surface free energies, interface free energy and lattice strain determine whether-or-not an epitaxial film will undergo 2-(layer-by-layer) or 3-(island) dimensional growth or a combination of initial layer-by-layer followed by island growth. The last phenomenon occurs in the case of pseudomorphic growths where the lattice parameters of the substrate and film are closely (not exactly) matched such that the film must be biaxially and elastically strained such that it comes into registry with the substrate. Continued deposition increases the total strain sufficiently such that 3-dimensional growth will occur. This latter phenomenon may also occur if there is interface mixing and/or surface reconstruction.

There is no known direct thermodynamic route to increase the surface energy of any substrate sufficiently such that this energy is greater than the sum of the surface energy of the diamond film + the diamond/substrate interfacial energy + the strain energy and, therefore, 2-dimensional nucleation and growth would occur. The surfactant route provides a thermodynamic route to solve a thermodynamic problem with a kinetic solution.

The thermodynamic problem is that a diamond nucleus without H on its surface wil not wet the surface of which we are aware. The thermodynamic route is the use of a surfactant which lowers the surface energy of both the substrate and the diamond film and which allows the diamond to retain the sp^3 bond at the surface of the growing film. The kinetic solution is that the C atoms which originally had sufficient mobility and time to form islands when C was deposited on a bare surface are now kinetically inhibited in terms of surface diffusion (since they are now covered by a capping layer) and in terms of chemical interdiffusion because the driving force of surface energy reduction via interdiffusion is now removed because they are no longer on the surface. However, if interfacial strain is created between the embedded layer and the substrate and, also, if the species of the embedded layer are soluble in the substrate under these conditions, interdiffusion should occur.

The substrate must be closely lattice matched (the lattice parameter of the film could be an integer multiple of that of the substrate). Thus, we are left with Ni, Cu, or cBN for the deposition of diamond, if we are to achieve 2-dimensional growth. Otherwise, the elastic strain will cause the

nucleation and growth to be 3-dimensional. Even with the use of a surfactant, the strain is not relieved enough to prevent 3-dimensional growth.

The selection of a good surfactant for the Ni or Cu substrates is rather limited. Getting the C underneath the surfactant and then getting it to form sp^3 bonds in the diamond crystal lattice on the surface of the substrate is going to be a problem. Ni or Cu or cBN are crystallographically close to diamond but the bonding is the question. Most any gaseous species should lower the surface energy of Cu or Ni and diamond and any monolayer of F or Cl would be a good choice at the moment. Since, a C containing gas species would not be able to get through the adsorbed gas without the common reactions that are currently being employed to achieve diamond, the best way may be to get the C to come to the surface from within the Cu or Ni. This has always created graphite during deposition or straight segregation.

Perhaps, as was mentioned by Max Yoder, if the metal was saturated with H and C at high temperature, annealed at lower temperature in a continuous flow of F or Cl or even H and see if the C will diffuse to and across the surface while connected to a gaseous species and tie up with other C species to give an sp^3 bond. Cu should be the best substrate in this case since the solubility of C is very low at all temperatures. The C would be introduced via implantation and the host crystal heated in a gradient so that the C will come to the desired surface. This method will be looked into with more detail in the near future.

Conclusion

As stated, the goal of this study is to achieve epitaxial growth of single crystal diamond films on one or more nondiamond substrates. The research vectors outlined above are: (a) high pressure, (b) ion beam enhanced epitaxy, and (c) the use of surfactants. The high pressure work will be done at Los Alamos National Laboratory under the guidance of Dr. Dave Schefferal and also Dr. Michael Paesler at NCSU. Sample preparation for the diamond anvil cell is already underway. The next step would be to send the samples with the amorphous C film to Dr. Bruce Sartwell for H-content determination and to Dr. James E. Butler for Raman analysis , who are both at the Naval Research Laboratory in Washington D.C..

The ion beam enhanced epitaxy project will be conducted at Oak Ridge National Laboratories under the supervision of Dr. Stephen Withrow. This project will be underway as soon as Dr. Withrow is able to get beam time. The surfactant project is still in the planning stages but once we find a suitable surfactant it will be underway.